ISSN: 26590530 Osinowo/JEAR 6 (1) (2023) 16-42

Journal of Earth and Atmospheric Research

# STATISTICAL STUDY OF WAVE HEIGHTS AND WIND SPEEDS IN THE BERMUDA SEA

Osinowo, A. A.

Department of Marine Science and Technology,
Federal University of Technology, Akure, Nigeria.

**Article History**
*Received: 15-04-21*
*Accepted: 29-05-23*

**Keywords:**
*significant wave height; occurrence; wind speed; sea state; trends*

## ABSTRACT

*The statistical characteristics of the Sea surface over the Bermuda Sea was investigated using a 37-year (1980–2016) daily significant wave height (SWH) and 10m wind speed data. In both cases, the slight and moderate Seas prevailed in the Sea. The Sea is generally rougher during winter. A spatial variation using SWH showed that higher frequencies (60%-85%) of the smooth (wavelets) to moderate Seas distribute around Turks and Caicos Islands, along the coasts of Albemarle Sound and western boundaries of the Sea. Much lower frequencies (0.06%-27%) of the rough to very high Seas distribute in the northeastern part of the Sea. The calm and phenomenal Seas are rare. Trends > 0.02m$\mathbf{yr}^{-1}$ for the smooth (wavelets) and high Seas are seen in few waters north of Albemarle Sound and Miami and in few regions in the central Bermuda Sea. Insignificant and negative trends occurred for the other Sea states. None of the Seas exhibited any significant increasing trend. Also, a spatial variation using u showed that higher occurrences (30%-60%) of the smooth (wavelets) to moderate Seas are seen in small regions in the central, southern and northern parts of the Sea. Lower frequencies (5%-28%) of the rough to very high Seas distribute in few regions in the southern and northern parts of the Sea, while the phenomenal Sea is very rare. Trends between 0.02ms$^{-1}$yr$^{-1}$ and 0.04ms$^{-1}$yr$^{-1}$ for the very rough Sea are seen in the extreme southwest of Bermuda Sea. The very high Sea showed trends > 0.2ms$^{-1}$yr$^{-1}$ in few waters in the south and all through the central and northern regions of the Sea. The phenomenal Sea exhibits the strongest positive trend of up to 5ms$^{-1}$yr$^{-1}$ in sporadic regions of the Sea. Insignificant and negative trends exist for the other categories of Sea.*

Correspondence: aaosinowo@futa.edu.ng

## 1 Introduction

Wave climate results from the interaction of the atmosphere and ocean. It is very important for several coastal engineering applications including the design and building of ports, offshore and coastal defense facilities, renewable energy harnessment, sediment transport, and coastal fluctuations. Since the surface winds are the main driving forces for wind waves, they are used in wave models to project wave climate under varying climate change scenarios. Based on this, many researchers used wind data from various GCMs to investigate wave characteristics and its prospective changes (*Hemer et al., 2013;*

*Kamranzad et al., 2015; Semedo et al., 2018;* Vanem, 2015; *Wandres et al., 2017; Wang et al., 2018).* Wave models are usually run through dynamical framework or through statistical means, each one having its own efficiency and short comings. The dynamical wave models, particularly the third generation wave models, e.g Wavewatch III Model have been extensively used for hindcasting and wave projection in many regions either for regional or global research *(Alizadeh et al. 2020; Hemer and Trenham 2016; Lemos et al. 2019;* Moeini and EtemadShahidi 2007; *Wandres et al. 2017).*

In projecting future wave climate, statistical approaches using regression models are widely used to establish a relationship between predictors including atmospheric variables and ocean wave heights as predictant *(Caires et al., 2006; Wang et al., 2014, 2010).*

MacHutchon, (2005) applied different methods of statistical analysis to the edge of the Agulhas Bank in the Southern Indian by using wave data collected over a period spanning from January 1998 to December 2003, on the Mossgas FA offshore gas drilling platform, on the Agulhas Bank in the Southern Indian Ocean. The study reveals that the Extreme 1 distribution applied to the study location.

A new statistical framework was employed by *Alizadeh et al (2021)* to achieve dependable wave forecasts in the Caspian Sea and also to manipulate various sources of uncertainty. They observed that the annual and seasonal variability of peak wave period and significant wave height do not change obviously as compared to the present climate. Moreover, wave energy analysis for the historical and future periods showed the sustainability of these promising renewable energy resources since clean energies are drawing much interest in meeting an increasing wants for electricity. The middle part of the southern Caspian Sea has abundance of energetic waves and this shows an higher potential for the utilization of energy than the western and eastern regions.

A global wave model was used by *Semedo et al. (2012)* to explore impacts of future warmer climate through A1B emission scenario. They reported increasing and decreasing trends in mean significant wave height respectively for lower and higher latitudes. The trends are stronger in the southern hemisphere compared to the northern hemisphere. *Casas-Prat et al. (2018)* employed WAVEWATCH III and GCM data of sea ice and wind (RCP8.5) to project global ocean wave climate. The study showed a decrease in wind speed and wave height in the North Atlantic and an increase in annual mean of wind speed, wave height and peak wave period in mid-high latitudes of the Southern Hemisphere. In addition, a large anticlockwise movement in the mean wave direction was observed in the Southern Hemisphere, which amounted to stronger waves migrating towards the Equator and turning into swells. This can be adduced as the major reason for increasing trends in wave height and period in the East Pacific and Indian Oceans, while decreasing trends for wind speeds are found in these areas.

Sea state refers to the overall condition of the sea surface following the impacts of swells, wind-

waves, and surface currents. In relation to the wave height and partly the wind speed, it can be explained as the amount of the roughness of the Sea surface. It can also be said to mean the effect that the local winds have on sea conditions – this is *independent* of traveling swell waves generated by winds outside of the local area. Sea state is related to the Beaufort scale which describes the state of the sea. The Beaufort wind force scale is an empirical measure that relates wind speed to observed conditions at sea. It was originally devised by an Irish Royal Navy officer, Francis Beaufort, in the early 19th century. In that time, naval officers made regular weather observations however without a standard scale, they were very subjective. The Beaufort scale assisted in standardizing these observations. The scale has been adjusted and added to over the past 200 years, and while some countries use forces up to seventeen, the World Meteorological Organization recognizes thirteen classes, from zero to twelve. Each Beaufort force number has expected wind speeds, wind wave heights and sea conditions associated with it. The Beaufort scale is very popular in the marine community as the condition of the sea is so important. A description of the sea surface is more beneficial to the mariner than just the wind wave heights alone. (https://blog.metservice.com.)

The World Meteorological Organization in 1929 adopted the Douglas Sea Scale after its advent in 1921. The scale, which ranges from 0 (calm) to 9 (confused) sea states is relatively correlated with the Beaufort Wind Scale. As suggested by the German Captain Petersen in 1939, a modification in Sea scale allowed for the evaluation of wind force from the Sea surface view. Hence, the Petersen Scale distinguished between the Douglas Sea Scale and Beaufort Wind Scale. In 1947, the World Meteorological Organization used an ocean wave code that varied slightly from the Douglas Sea Scale.

Statistical explanation of sea conditions basically necessary for design of marine structures and management of marine operations is strongly dependent on the analysis of long term wave data. To create such a long-term statistical description of sea states, hindcast datasets, visual observations and wave measurements (both remote sensing and in-situ,) are widely used. The meaning of sea states danger relies on the particular application, for example, steep sea states are unsafe for capsizing of small vessels. They can be critical for parametric roll *(Bitner-Gregersen et al., 2016).*

A common idea related to field observations of sea states has been given by *Ardhuin et al., (2019)*, stating that field observations can be supplemented with estimates along the path of a ship using the wave buoy analogy (Nielsen 2017, Nielsen and Dietz, 2020.) where the ship itself can be a wave sensor.

With escalating shipping operations, navigation security is a major issue, particularly when economic losses, human casualties and environmental issues are taken into account. The sea surface conditions play an important part in shipping safety. However, the types of risky sea states that cause severe shipping accidents are not well understood. Zhang and Li, (2017) analyzed the sea state characteristics during ship accidents that happened in poor weather or heavy seas,

using a ten-year ship accident dataset. The sea state variables, which include the significant wave height, mean wave period and mean wave direction, got from numerical wave model data were analyzed for some chosen ship accidents. The results showed that complex sea conditions with the co-occurrence of wind sea and swell conditions pose threats to sailing vessels, particularly when these conditions include close wave periods and oblique wave directions.

*Innocenti et al., (2021)* used the Higher Order Spectral Method to analyze a number of sea-states that occurred in a region in the Mediterranean sea, close to the location of a reported accident, with the aim of relating the likelihood of extreme conditions with varying sea state conditions. They found that the case study of the reported accident was not amongst the most dangerous.

*Dodet et al., (2020)* implemented the first release of the Sea State Climate Change Initiative (CCI) dataset, the execution and advantages of a complex denoising method, its justification against field observations and numerical model outputs, and the prospects considered within the Sea State CCI project.

An approach based on simulation methods for fluctuation categorizations of unmanned surface vehicle (USV) functionalities under the slight sea conditions (Sea State 3) was proposed by *Park et al., (2017)*. They concluded that the design specifications like maximum velocity, acceleration and range of motion could be evaluated using the simulation data.

Higher sea states are of significant importance to mariners and seabed drilling operators in the region, for whom the particular sea condition can raise the possibility of hazardous icing conditions on ships and structures *(Thompson et al., 2016).*

With the aim of carrying out an all-year marine process like the sub-Sea fittings and intervention, drilling, and pipe laying in rough Seas, *Nguyen et al., (2007)* integrated suitable controllers at the plant control level into a hybrid DP system so as to run from calm to extreme Sea conditions. Phenomenal Seas, regarded by the World Meteorological Organization as having a significant wave height more than 14 m, were examined by *Hanafin et al., (2012)* over the North Atlantic Ocean in February 2011. They reported that phenomenal Sea states from storm Quirin were sensed by satellites, and gave extremely long swells along the western coast of Europe, which were observed by wave buoys and seismic stations. Sea surface conditions between the storm source and swell landfall can be estimated using numerical wave models, while a state-of-the-art model, WAVEWATCH-III (WW3), was engaged to reproduce both the extreme Sea surface conditions and ensuing swell fields produced by this storm.

By utilizing a 6-hourly averaged numerically simulated daily wave height and wind speed data over a 30-year period, the statistical description of Sea conditions in the South China Sea was studied by *Osinowo et al., (2017)*. They reported that the slight Sea state prevailed over the location and had almost the largest occurrence in all Seasons and monthly SWH. The study revealed that the moderate Sea condition occurred mostly in December and January, while the smooth

(wavelets) Sea state had the highest frequency in May. The calm and smooth Sea states had higher frequencies (25%-80%) in the southern area of the Sea.

Until recently, the statistical attributes of mixed Sea states over the Bermuda Sea have not yet been well investigated. Analysis of the Sea surface conditions serves as a reference tool for the wave energy resources development, navigation, marine engineering, disaster prevention and reduction.

Bermuda Triangle, section of the North Atlantic Ocean off North America has a vaguely triangular shape marked by the Atlantic coast of the Florida panhandle (in the United States), Bermuda, and the Greater Antilles (https://www.britannica.com). There is no doubt this area is prone to rogue waves," Simon Boxall, an oceanographer at the University of Southampton and one of the scientists on the team, told Live Science. They are possible "anywhere you get multiple storms coming together. "Rogue waves are steep and tall, like "walls of water," and they often hit unexpectedly, according to the National Oceanic and Atmospheric Administration. The tip of South Africa, for example, is very prone to them, where waves from storms in the South Atlantic Ocean, the Indian Ocean and the Southern Ocean all come together at once, Boxall said. Indeed, there were similar disappearances of big container vessels and tankers off the tip of South Africa throughout the years, he said. This also holds true for the Bermuda Triangle, where storms can come from all directions, like Mexico, the equator and farther east in the Atlantic. If each wave can reach over 30 feet (10 meters) tall, occasionally they can coincide at the right moment and create a rogue, or "freak," wave that can be over 100 feet (30 m) high. (https://www.livescience.com)

A statistical approach is employed in this study to characterize the sea surface conditions of the study region and to extend the work by *Osinowo et al., (2018)* in investigating the spatial trends in the different Sea states, using numerically simulated data sets of the SWH and 10m wind speed from 1980 to 2016.

This paper is structured as follows: The wave model setup and a comprehensive validation with buoy data with some statistical tests and their results are contained in Section 2. The methodologies used in characterizing the Sea conditions and an in-depth discussion of results obtained are all presented in Section 3. Finally, paper is concluded in Section 4.

## 2. Models, data sets and methodology

### 2.1 The wave model and input data

The version 3.14 of the third-generation spectral wave model WAVEWATCH III ™ (WW3), which accounts for wind input, wind-wave interaction, and dissipation due to whitecapping and wave-bottom interaction was used to simulate ocean wave parameters over the Bermuda Sea (Figure. I). The wave model was built up at the Ocean Modeling Branch of the Environmental Modeling Center of the National Center for Environmental Prediction (NCEP) for ocean wave forecasts. It was developed from Wavewatch-I and Wavewatch-II at the Delft University of

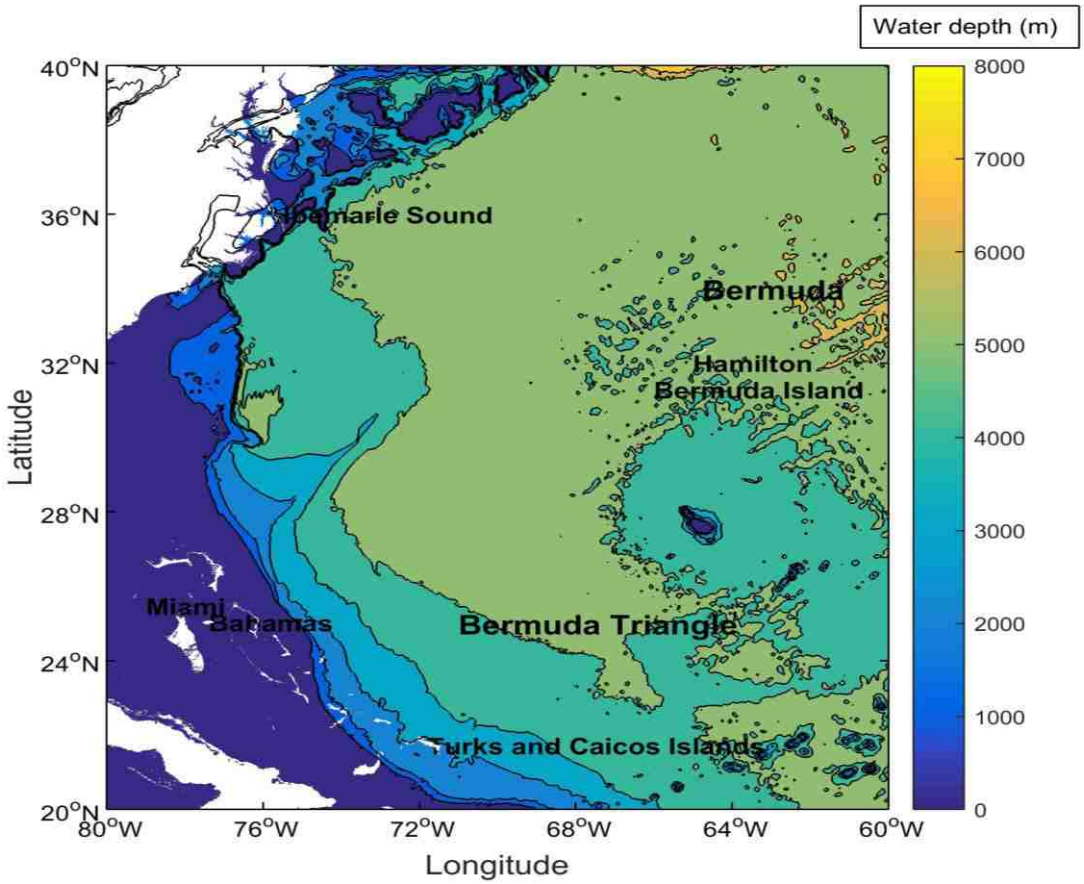



**Figure. I** Topography of the Bermuda Sea and surrounding waters.

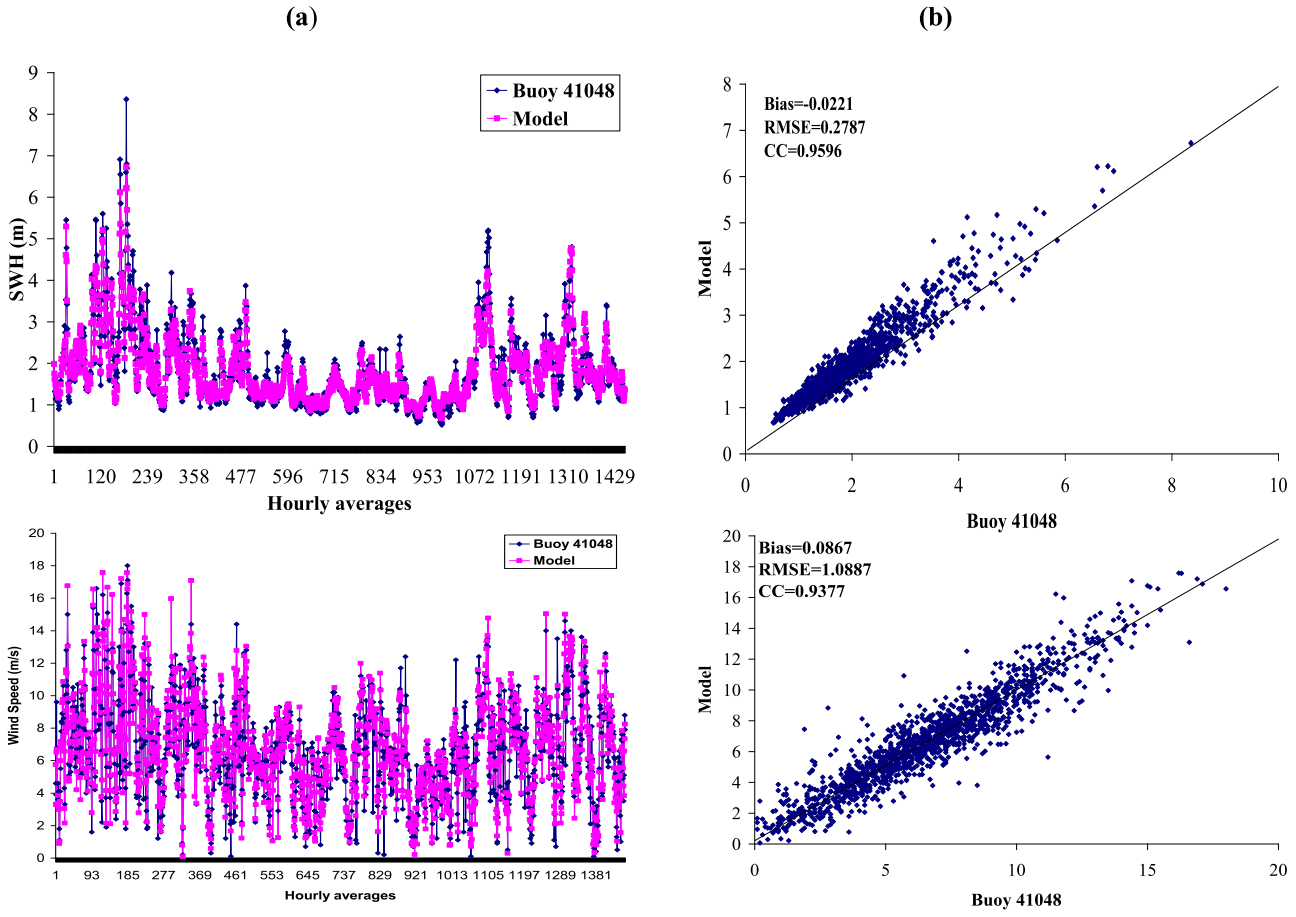
Technology, and NASA Goddard Space Flight Center, respectively (Tolman, 2009). By using the National Geophysical Data Center (NGDC) one minute Bathymetric, Topographic/Elevation (ETOP 01) data, with a resolution of 0.017 ° × 0.017 °, the water depth field over the study location defined by coordinates 80°W-60°W and 20°N-40°N and which was processed by the Gridgen 3.0 packet was obtained. Source terms for energy spectra in the model, which use wind-wave interaction (Chalikov and Belevich, 1993, Tolman and Chalikov, 1996, Tolman 1999), the discrete interaction approximation (DIA) for nonlinear interactions (as in WAM), and bottom friction as in the Joint North Sea Wave Project (JONSWAP) are all set to default. The model integrates the spectrum to a cut-off frequency, and above this frequency a parametric tail is applied. The boundary condition is cyclical. The other option settings are 36 directions, and 24 discrete wave-numbers (0.0412 ~ 0.4060Hz, 2.4 ~ 24.7s).

The model spatial grid covers the study location from 80°W-60°W and 20°N-40°N at $0.017^0$ resolution. The model in an operational/forecasting mode, uses a time step of 3600 s, and was forced with 6-hour re-analysis 10m wind fields, extracted over 90°W-50°W and 10°N-50°N from the European Center for Medium Range Weather Forecast (ECMWF) ERA-Interim from 1980 to 2016 on a $0.125^0$ (longitude) by $0.125^0$ (latitude) Gaussian grid. The

model output is a two-dimensional (2D) wave energy spectra obtained at each grid point with period spanning from 1st January, 1980 to 31st December, 2016 and providing a 6-hour averaged, daily output wave parameters including wave spectra, SWH ($4\sqrt{E}$), mean wavelength ($2\Pi k^{-1}$), mean wave period ($2\Pi/\omega$), mean wave direction, peak frequency, and peak direction where E, k and ω are respectively the total spectral energy, wave number and angular frequency. Two thousand (2000) points were randomly selected within the Bermuda Sea. The simulation provided a time series of SWH and other wave parameters over 1832 water points. The rest 168 land points were sieved out from the data to be analyzed.

## 2.2 Data Validation

Figure II shows the comparisons conducted between observations and simulations for significant wave height and wind speed for year 2015. Buoy (observational) data were obtained from the National Data Buoy Center (NDBC) for buoy 41048 in West Bermuda, coordinates 31.86$^0$N, 69.59$^0$W and buoy 41049 in South Bermuda, coordinates 26.537$^0$N, 62.945$^0$W which are buoy locations in the Bermuda Sea. The corresponding SWH and wind speed data were computed by the model over the buoy coordinates. There is good agreement between observations and simulations on the curve trends.



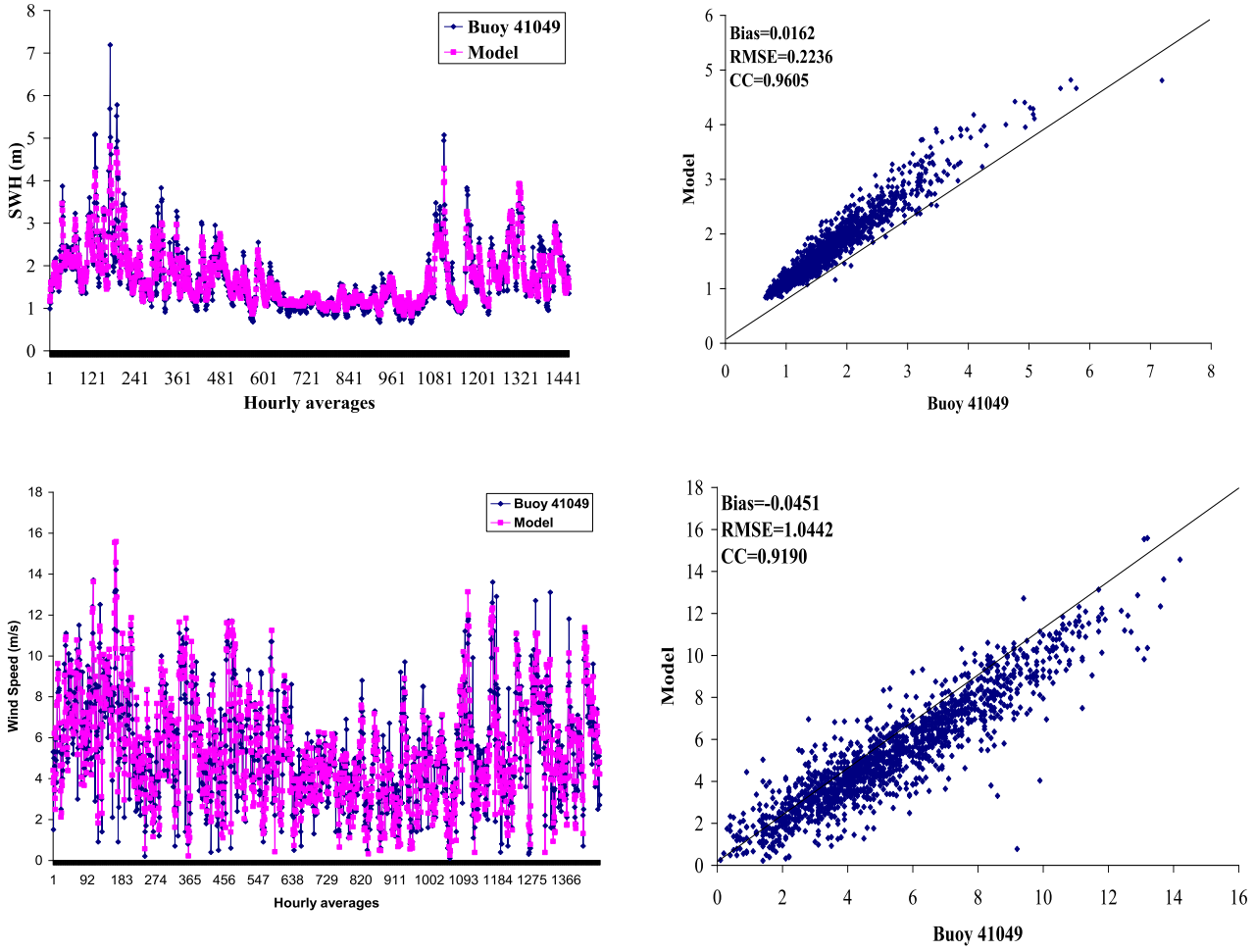



**Figure. II** (a) Time series (from 01 Jan 2015 to 31 Dec 2015) and (b) scatter plots of a model against buoy data for the SWH and wind speed for buoys 41048 and 41049. On the x-axis is the number of data points.

The accuracy of the wind and wave parameters computed by the model was evaluated through a conventional statistical analysis that consists of calculating the following in Wilks, (1995):

$$cc = \frac{\sum_{i-1}^{n}(x_i - \bar{x})(y_i - \bar{y})}{\sqrt{\sum_{i-1}^{n}(x_i - \bar{x})^2 \sum_{i-1}^{n}(y_i - \bar{y})^2}} \quad (1)$$

$$Bias = \bar{y} - \bar{x} \quad (2)$$

$$RMSE = \sqrt{\frac{1}{N}\sum_{i-1}^{n}(y_i - x_i)^2} \quad (3)$$

Where, $x_i$ represents the buoy data, $y_i$ represents the model data, x and y are mean values of buoy and model data, N is the total number of observations.

As shown in Figure II b, it is clear that the parameters computed by the model and their observed values are highly correlated with the correlation coefficient (cc) larger than 0.9 for all the cases and significant at the 99% level. The calculated mean bias error (MBE) ranged between -0.045m/s and 0.087m/s, while the root mean square error (RMSE) ranged between 0.224m and 1.089m/s .

**Table 1.** Douglas Sea state scale for SWH and Wind Speed.

| Sea State Code | SWH | Wind Speed | Characteristics |
|---|---|---|---|
| 0 | 0 metres (0 ft) | | Calm (glassy) |
| 1 | 0 to 0.1 metres (0.00 to 0.33 ft) | | Calm (rippled) |
| 2 | 0.1 to 0.5 metres (3.9 in to 1 ft 7.7 in) | < 3.598 m/s | Smooth (wavelets) |
| 3 | 0.5 to 1.25 metres (1 ft 8 in to 4 ft 1 in) | 3.598 to 6.168 m/s | Slight |
| 4 | 1.25 to 2.5 metres (4 ft 1 in to 8 ft 2 in) | 6.168 to 8.224 m/s | Moderate |
| 5 | 2.5 to 4 metres (8 ft 2 in to 13 ft 1 in) | 8.224 to 9.766 m/s | Rough |
| 6 | 4 to 6 metres (13 to 20 ft) | 9.766 to 11.822 m/s | Very rough |
| 7 | 6 to 9 metres (20 to 30 ft) | 11.822 to 15.42 m/s | High |
| 8 | 9 to 14 metres (30 to 46 ft) | 15.42 to 23.13 m/s | Very high |
| 9 | Over 14 metres (46 ft) | > 23.13 m/s | Phenomenal |

In general, the simulation results are consistent with the observations, which show that WW3 can well reproduce the wind-wave parameters and represents a reliable model to model surface wave in the Bermuda Sea.

### 2.3 Analysis of Sea surface conditions

The monthly variations of SWH and wind speed in Figure III showed that both variables have minimum values in June through August with respective values of 1.22m, 1.2m and 1.23m for the SWH and 5.52ms$^{-1}$, 5.63ms$^{-1}$ and 5.29 ms$^{-1}$ for the wind speed. Their maximum values occurred in January and February with respective values of 2.23m and 2.22m for the SWH and 7.87ms$^{-1}$ and 7.83ms$^{-1}$ for the wind speed. The WW3 model has been set to output several parameters at 6-hourly

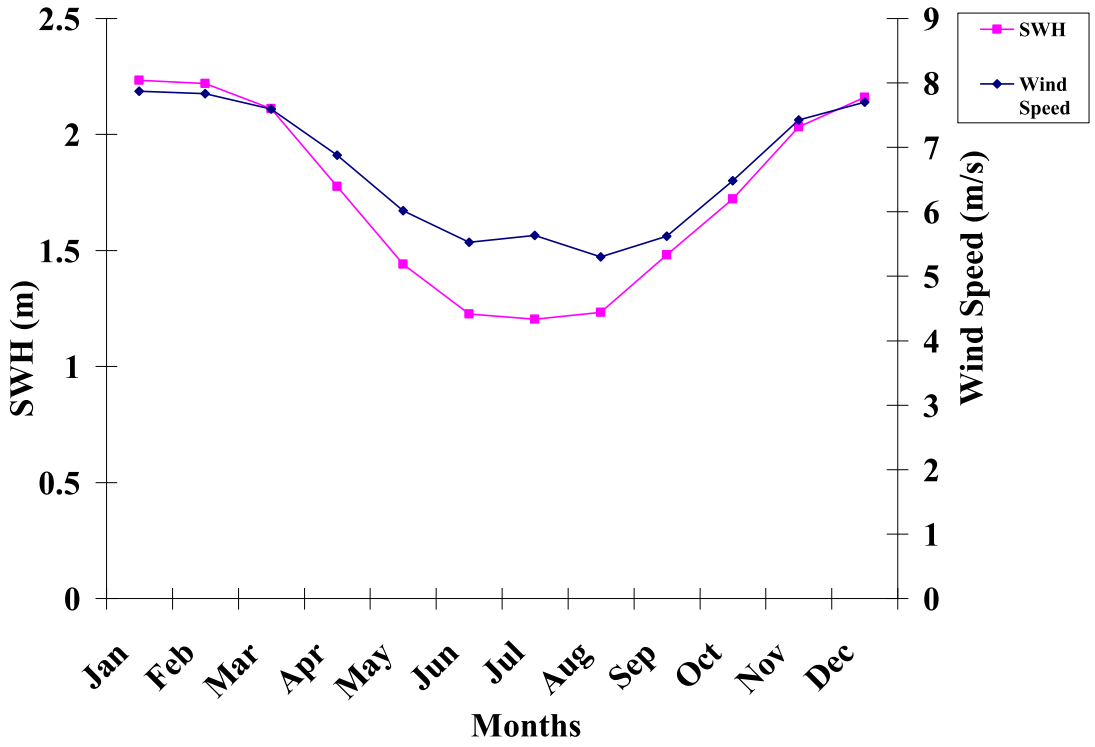



**Figure. III**. Monthly variation of SWH and Wind Speed in the Bermuda Sea.

intervals for the 37-year hindcast. Out of the main output parameters, the SWH and wind speed were used to characterize the Sea conditions in the Bermuda Sea. The monthly variation of SWH with wind speed in the Bermuda Sea were analyzed and shown in Figure III. For the different categories of Sea states and for the different range of SWH shown in Table 1, the information on the annual, Seasonal and monthly mean Sea states in the Bermuda Sea is presented as cumulative frequency f(SWH) in percentage as:

$$f(SWH) = 100(n/N) \text{----------} (4)$$

Where n is the frequency of SWH that satisfies each of the defined range of SWH for the various Sea states and N is the total number of SWH values. Also, for the different categories of Sea states and for the different range of u shown in Table 1, the information on the annual, Seasonal and monthly mean Sea states in the Bermuda Sea is presented as cumulative frequency f(u) in percentage as:

$$f(\text{wind speed}) = 100(n/N) \text{----------} (5)$$

Where n is the frequency of wind speed that satisfies each of the defined range of wind speed for the various Sea states and N is the total number of wind speed values.

The Seasonal mean Sea state characterization was determined by combining: the November-March monthly mean Sea states for winter and April-October for summer. The Seasonal and monthly mean Sea states are presented in Tables 2 and 3 respectively for the SWH and wind speed. Also, for a spatial distribution, the percentage cumulative frequency of the SWH and wind speed

**Table II.** Average Seasonal and monthly SWH values (in m) for the Bermuda Sea (*f* is computed using Equation 4).

| Season | SWH=0 | SWH≤0.1 | 0.1≤SWH≤0.5 | 0.5≤SWH≤1.25 | 1.25≤SWH≤2.5 | 2.5≤SWH≤4.0 | 4.0≤SWH≤6.0 | 6.0≤SWH≤9.0 | 9.0≤SWH≤14.0 | SWH≥14.0 |
|---|---|---|---|---|---|---|---|---|---|---|
| Summer | 0 | 0.03 | 1.70 | 44.59 | 47.24 | 5.57 | 0.77 | 0.09 | 0.00 | 0 |
| Winter | 0 | 0.02 | 0.81 | 14.10 | 57.09 | 22.17 | 5.19 | 0.61 | 0.01 | 0 |
| Month | SWH=0 | SWH≤0.1 | 0.1≤SWH≤0.5 | 0.5≤SWH≤1.25 | 1.25≤SWH≤2.5 | 2.5≤SWH≤4.0 | 4.0≤SWH≤6.0 | 6.0≤SWH≤9.0 | 9.0≤SWH≤14.0 | SWH≥14.0 |
| Jan | 0 | 0.02 | 0.80 | 12.75 | 55.31 | 24.21 | 6.28 | 0.64 | 0.00 | 0 |
| Feb | 0 | 0.02 | 0.81 | 13.33 | 55.71 | 22.69 | 6.62 | 0.81 | 0.02 | 0 |
| Mar | 0 | 0.01 | 0.91 | 15.93 | 55.89 | 21.75 | 4.85 | 0.64 | 0.02 | 0 |
| Apr | 0 | 0.01 | 1.20 | 23.30 | 61.12 | 12.30 | 1.90 | 0.17 | 0.00 | 0 |
| May | 0 | 0.02 | 1.69 | 41.20 | 51.72 | 4.85 | 0.50 | 0.02 | 0.00 | 0 |
| Jun | 0 | 0.03 | 2.14 | 59.38 | 36.57 | 1.79 | 0.09 | 0.00 | 0.00 | 0 |
| Jul | 0 | 0.04 | 1.84 | 60.62 | 36.48 | 0.98 | 0.04 | 0.00 | 0.00 | 0 |
| Aug | 0 | 0.05 | 1.96 | 60.73 | 34.99 | 1.91 | 0.32 | 0.04 | 0.00 | 0 |
| Sep | 0 | 0.03 | 1.82 | 41.38 | 49.38 | 6.23 | 0.97 | 0.18 | 0.00 | 0 |
| Oct | 0 | 0.03 | 1.30 | 25.23 | 60.59 | 11.04 | 1.59 | 0.21 | 0.01 | 0 |
| Nov | 0 | 0.03 | 0.77 | 15.15 | 60.59 | 19.93 | 3.20 | 0.32 | 0.01 | 0 |
| Dec | 0 | 0.02 | 0.74 | 13.29 | 57.96 | 22.27 | 5.09 | 0.64 | 0.00 | 0 |
| Avg | 0 | 0.02 | 1.33 | 31.86 | 51.36 | 12.50 | 2.62 | 0.31 | 0.01 | 0 |

for the different categories of Sea states were computed for each grid point of the Bermuda Sea domain and surrounding regions.

## 3.0 Results and discussion.

### 3.1 Sea states characterization using SWH

The annual, Seasonal, and monthly mean cumulative percentages of frequency for different Seas states using the SWH are as shown in Figures IV-VI . For the annual mean characterization (Figure IV), the moderate Sea has the highest percentage occurrence of 51.32% all through the Bermuda Sea. The occurrences of smooth (wavelets), slight, rough and very rough Seas with respective frequencies of 1.33%, 31.96%, 12.45% and 2.6% are smaller. Hardly is the Sea condition in the Bermuda Sea in the calm (glassy), calm (rippled) high, very high and phenomenal states.




**Figure IV.** Annual mean cumulative percentage frequency of *SWH* for the different Sea states in the Bermuda Sea.

**Table III.** Average Seasonal and monthly wind speed values (in m/s) for the Bermuda Sea (*f* is computed using Equation 5).

| Season | wind speed<3.598 | 3.598≤wind speed≤6.168 | 6.168≤wind speed≤8.224 | 8.224≤wind speed≤9.766 | 9.766≤wind speed≤11.822 | 11.822≤wind speed≤15.42 | 15.42≤wind speed≤23.13 | wind speed>23.13 |
|---|---|---|---|---|---|---|---|---|
| Summer | 20.81 | 36.00 | 24.86 | 9.88 | 5.57 | 2.44 | 0.42 | 0.01 |
| Winter | 11.50 | 24.16 | 23.95 | 15.08 | 13.25 | 9.61 | 2.43 | 0.02 |

| Month | wind speed<3.598 | 3.598≤wind speed≤6.168 | 6.168≤wind speed≤8.224 | 8.224≤wind speed≤9.766 | 9.766≤wind speed≤11.822 | 11.822≤wind speed≤15.42 | 15.42≤wind speed≤23.13 | wind speed>23.13 |
|---|---|---|---|---|---|---|---|---|
| Jan | 11.13 | 23.12 | 23.40 | 14.90 | 13.45 | 11.02 | 2.96 | 0.02 |
| Feb | 11.26 | 23.98 | 23.29 | 14.35 | 13.10 | 11.00 | 2.97 | 0.04 |
| Mar | 11.99 | 24.90 | 23.91 | 14.59 | 12.85 | 9.37 | 2.36 | 0.03 |
| Apr | 14.62 | 29.31 | 25.56 | 13.72 | 10.16 | 5.59 | 1.04 | 0.00 |
| May | 19.74 | 34.77 | 25.65 | 11.15 | 6.09 | 2.31 | 0.29 | 0.00 |
| Jun | 23.02 | 39.43 | 24.42 | 8.04 | 3.75 | 1.25 | 0.10 | 0.00 |
| Jul | 20.38 | 39.19 | 27.32 | 9.03 | 3.34 | 0.69 | 0.05 | 0.00 |
| Aug | 25.92 | 39.73 | 23.57 | 7.03 | 2.70 | 0.84 | 0.18 | 0.01 |
| Sep | 24.21 | 37.91 | 22.99 | 7.79 | 4.36 | 2.16 | 0.55 | 0.03 |
| Oct | 17.75 | 31.65 | 24.50 | 12.43 | 8.60 | 4.29 | 0.77 | 0.02 |
| Nov | 11.80 | 24.97 | 25.00 | 15.95 | 13.33 | 7.56 | 1.38 | 0.01 |
| Dec | 11.30 | 23.81 | 24.11 | 15.58 | 13.52 | 9.17 | 2.51 | 0.01 |
| Avg | 16.93 | 31.06 | 24.48 | 12.05 | 8.77 | 5.44 | 1.26 | 0.02 |

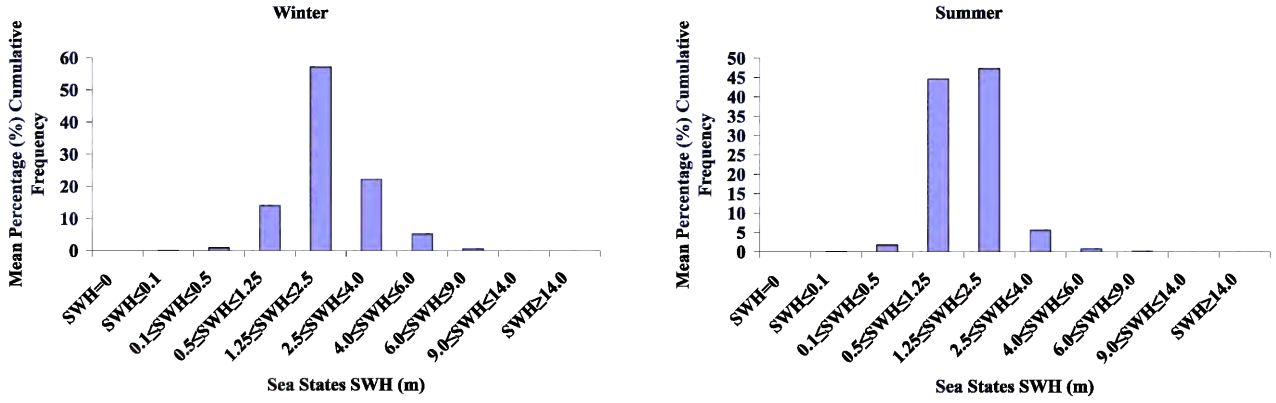
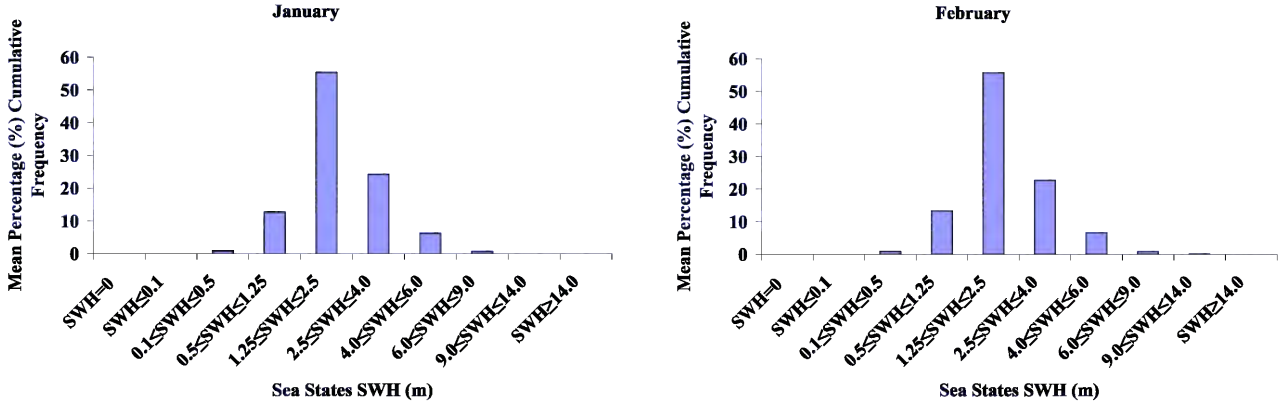
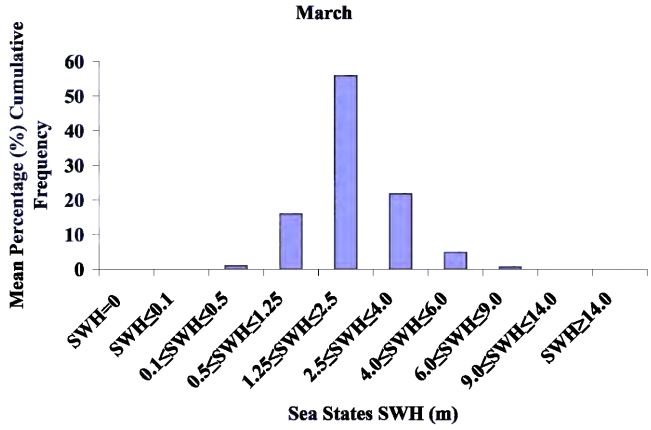
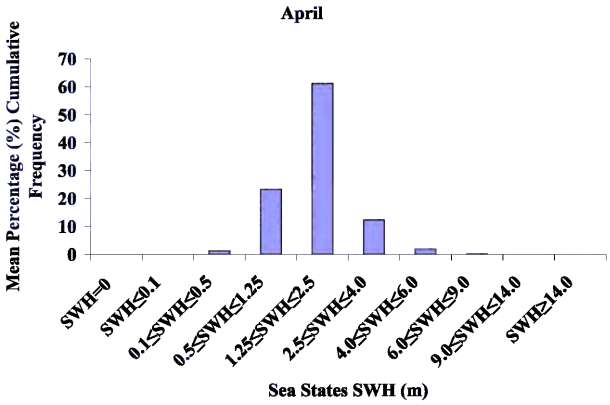
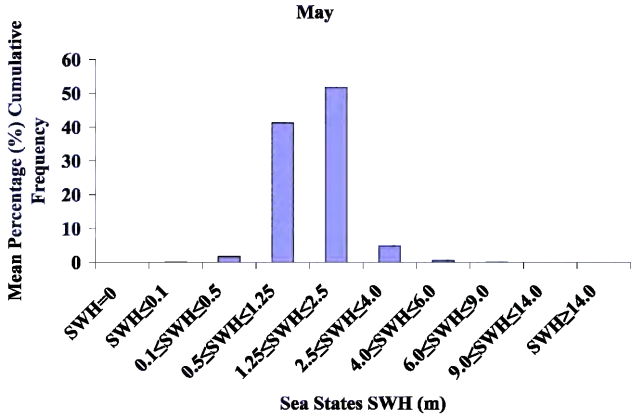


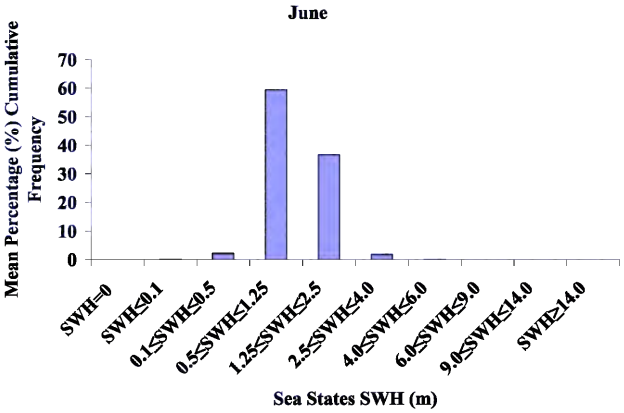

**Figure V.** Seasonal mean cumulative percentage frequency of *SWH* for the different Sea states in the Bermuda Sea.

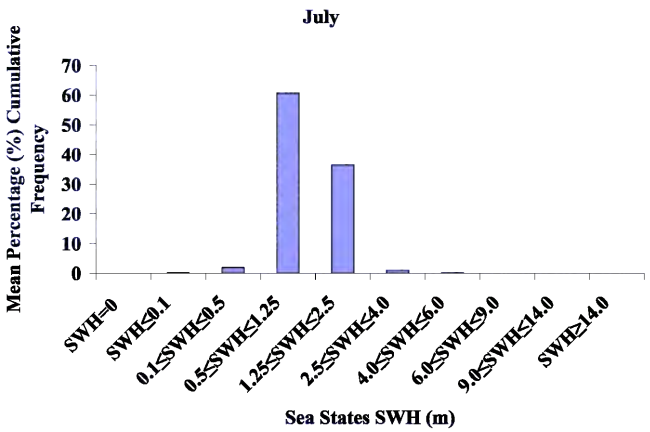


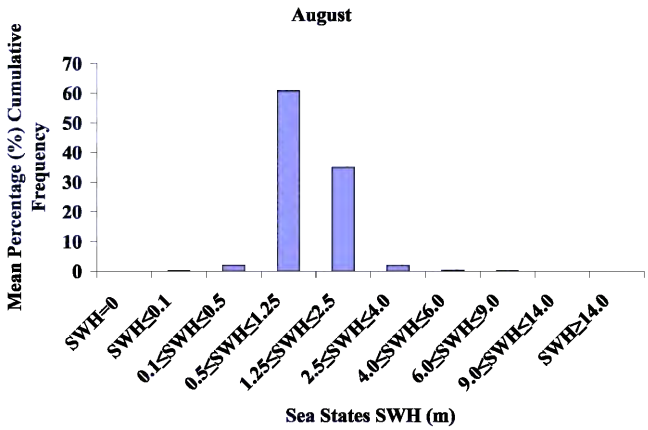

March
Mean Percentage (%) Cumulative Frequency
0
10
20
30
40
50
60
SWH=0
SWH≤0.1
0.1≤SWH≤0.5
0.5≤SWH≤1.25
1.25≤SWH≤2.5
2.5≤SWH≤4.0
4.0≤SWH≤6.0
6.0≤SWH≤9.0
9.0≤SWH≤14.0
SWH≥14.0
Sea States SWH (m)


April
Mean Percentage (%) Cumulative Frequency
0
10
20
30
40
50
60
70
SWH=0
SWH≤0.1
0.1≤SWH≤0.5
0.5≤SWH≤1.25
1.25≤SWH≤2.5
2.5≤SWH≤4.0
4.0≤SWH≤6.0
6.0≤SWH≤9.0
9.0≤SWH≤14.0
SWH≥14.0
Sea States SWH (m)


May
Mean Percentage (%) Cumulative Frequency
0
10
20
30
40
50
60
SWH=0
SWH≤0.1
0.1≤SWH≤0.5
0.5≤SWH≤1.25
1.25≤SWH≤2.5
2.5≤SWH≤4.0
4.0≤SWH≤6.0
6.0≤SWH≤9.0
9.0≤SWH≤14.0
SWH≥14.0
Sea States SWH (m)


June
Mean Percentage (%) Cumulative Frequency
0
10
20
30
40
50
60
70
SWH=0
SWH≤0.1
0.1≤SWH≤0.5
0.5≤SWH≤1.25
1.25≤SWH≤2.5
2.5≤SWH≤4.0
4.0≤SWH≤6.0
6.0≤SWH≤9.0
9.0≤SWH≤14.0
SWH≥14.0
Sea States SWH (m)


July
Mean Percentage (%) Cumulative Frequency
0
10
20
30
40
50
60
70
SWH=0
SWH≤0.1
0.1≤SWH≤0.5
0.5≤SWH≤1.25
1.25≤SWH≤2.5
2.5≤SWH≤4.0
4.0≤SWH≤6.0
6.0≤SWH≤9.0
9.0≤SWH≤14.0
SWH≥14.0
Sea States SWH (m)


August
Mean Percentage (%) Cumulative Frequency
0
10
20
30
40
50
60
70
SWH=0
SWH≤0.1
0.1≤SWH≤0.5
0.5≤SWH≤1.25
1.25≤SWH≤2.5
2.5≤SWH≤4.0
4.0≤SWH≤6.0
6.0≤SWH≤9.0
9.0≤SWH≤14.0
SWH≥14.0
Sea States SWH (m)

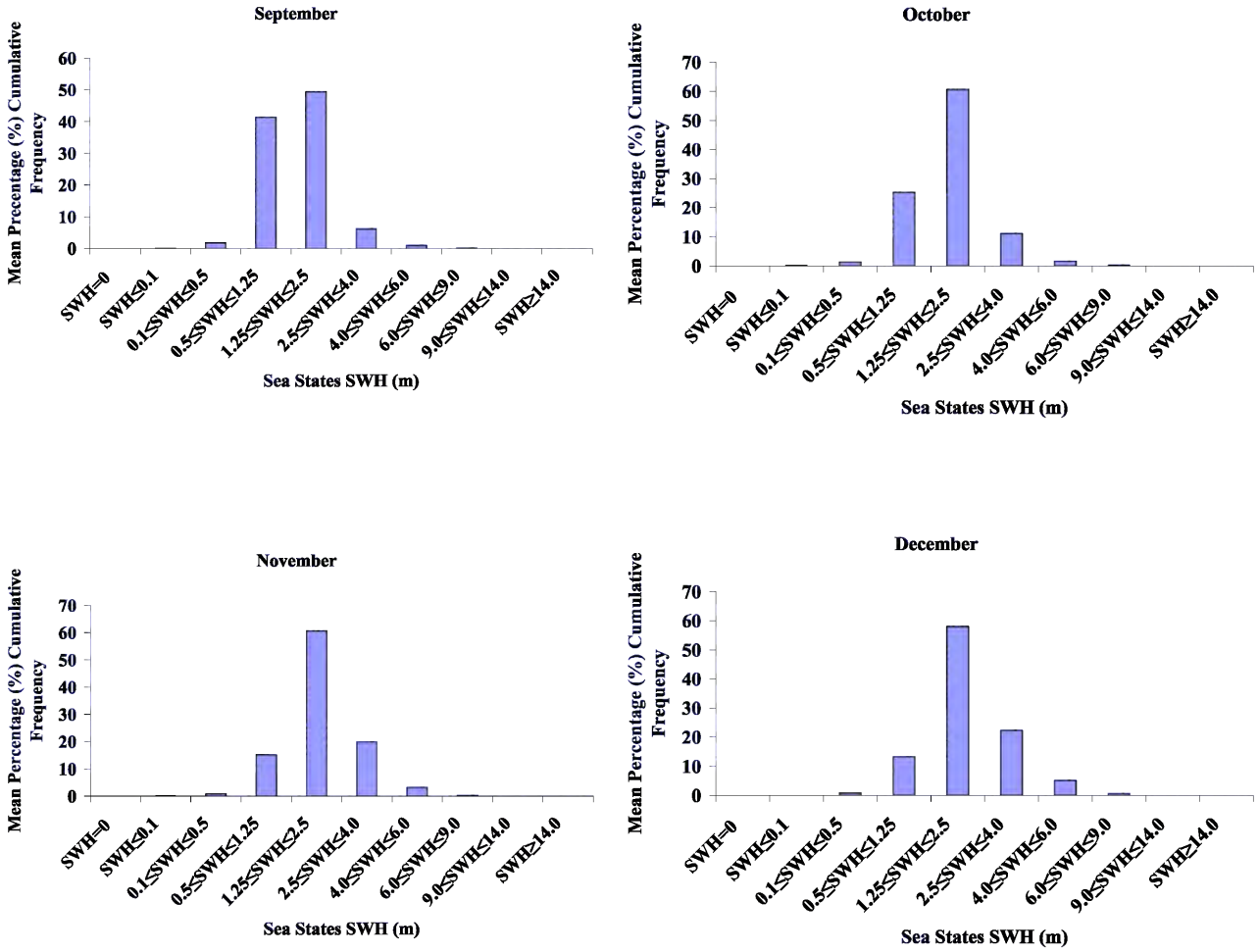



**Figure VI.** Monthly mean cumulative percentage frequency of *SWH* for the different Sea states in the Bermuda Sea.

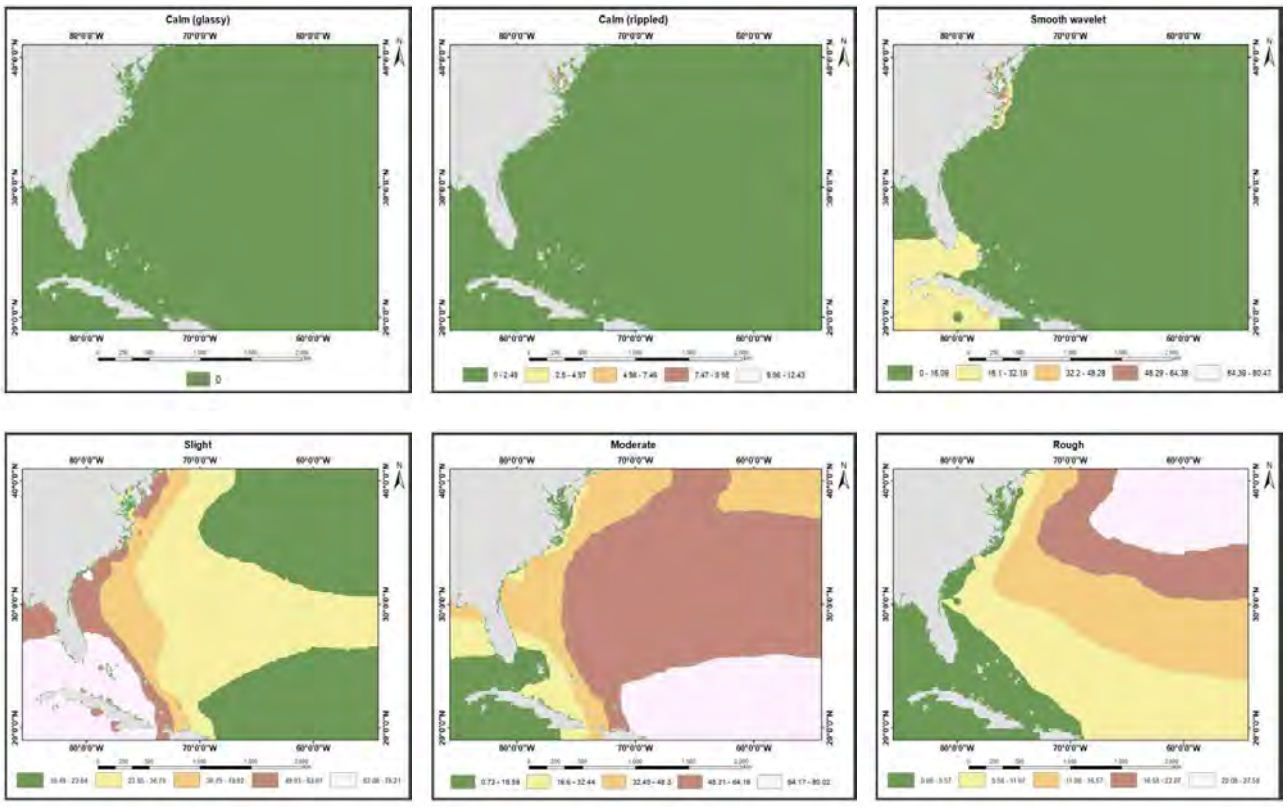
For the Seasonal Sea surface characteristics presented in Figure.V, the moderate Sea has the largest percentage frequencies of 57.1% and 47.24% both at winter and summer. The percentage frequencies of the smooth (wavelets) and slight Seas with respective frequencies of 1.71% and 44.6% are higher during summer than in winter. Higher percentage frequencies, especially for the rough (22.2%) and very rough (5.2%) Seas suggest that the Sea appears to be rougher during winter. For both Seasons, hardly is the Sea condition in the calm (glassy), calm (rippled), high, very high and phenomenal states.

The monthly mean characterization in Figure.VI shows that the moderate Sea generally has higher occurrence in all months except in June through August in which the slight Sea had higher frequencies which are respectively 59.38%, 60.63% and 60.73%. The moderate Sea occurred most (61.12%) in April and occurred least (34.98%) in August. From November through March, the rough Sea showed higher frequencies than the slight Sea. Higher occurrences exist for the slight Sea during April through October.

The very rough Sea had higher frequencies in December through February with respective values of 5.09%, 6.28% and 6.62%. The calm (rippled), high and very high Seas occurred on rare occasions. In all the months, the calm (glassy) and phenomenal Seas had no occurrence.

### 3.2 Spatial Distribution of Sea States Using SWH

Figure VII presents the spatial characteristics of the cumulative percentage frequencies of SWH for the different Sea conditions. It is observed that the smooth (wavelets) Sea showed little occurrence (8% -35%) in waters surrounding Miami and Bahamas. The frequency is largest (70% -85%) along the coasts of Albemarle Sound. The slight Sea increased westwards and had peak frequencies (60% -75%) along the western boundaries of the Sea. The occurrence of the moderate Sea increased southwards and had the highest occurrence (70% -80%) around Turks and Caicos Islands. Least occurrences of less than 35% distribute along the western boundaries of the Sea. As regards the frequency distribution of the rough and very rough Seas, higher frequencies (20% -27%) of the rough Sea occupied larger waters in the northeastern part of the Sea as compared to the higher frequencies (8% -11%) of very rough Seas in the northeastern waters. Higher frequencies exist for the high (1.75% -2.25%) and very high (0.06% -0.08%) Seas in sporadic waters in the northeastern part of the Sea. The calm (glassy), calm (rippled) and phenomenal Seas showed very little or no occurrence



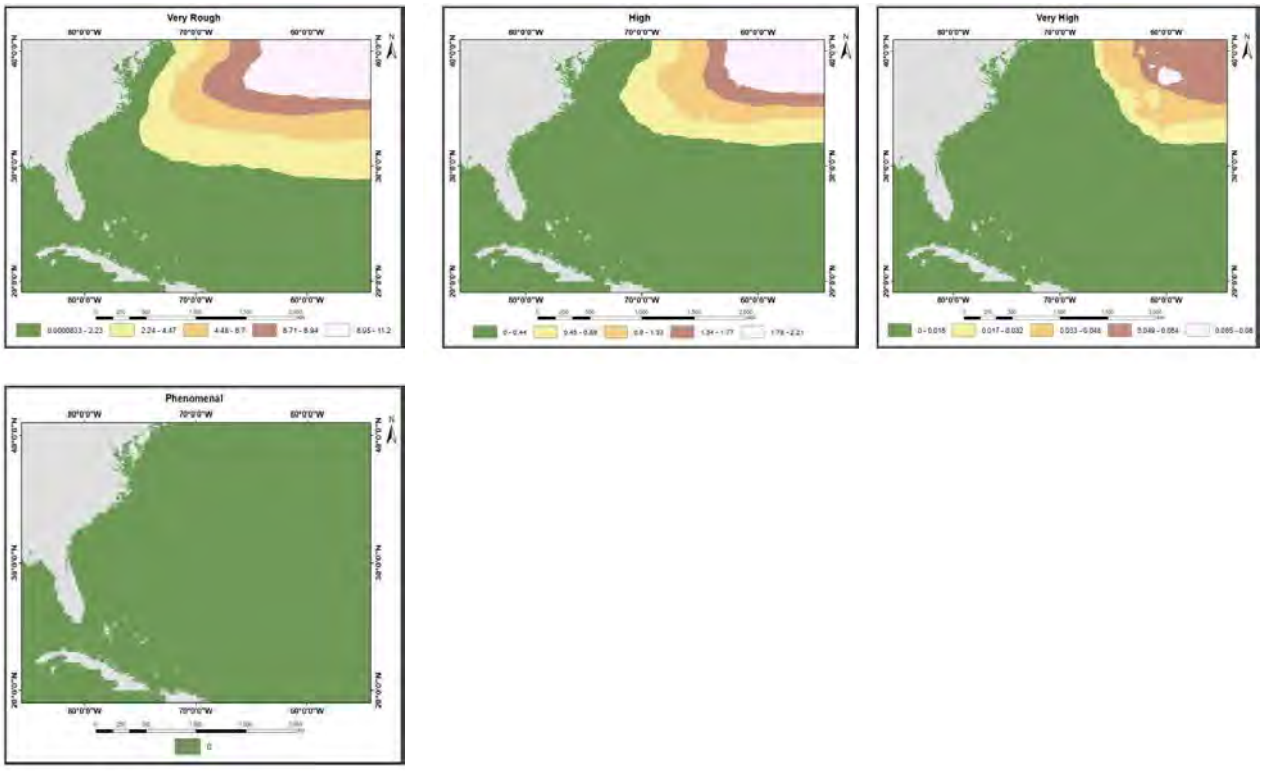



**Figure VII.** Spatial variation of the cumulative percentage frequency of *SWH* for the various Sea states in the Bermuda Sea. Values on the vertical bars are in percentage.

### 3.3 Sea states characterization using wind speed

The annual, Seasonal and monthly mean cumulative percentages of frequency for different Seas using wind speed are shown in Figures. VIII-X. For the annual mean characterization (Figure.VIII), the slight Sea has the highest percentage occurrence of 31.1% all through the Bermuda Sea. The occurrences of the smooth

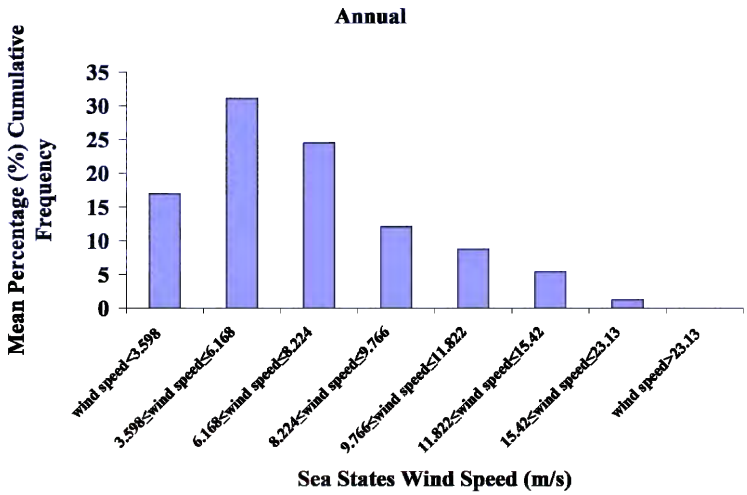



**Figure. VIII**. Annual mean cumulative percentage frequency of *wind speed* for different Sea states in the Bermuda Sea

(wavelets), moderate, rough, very rough and high Seas are respectively 16.95%, 24.48%, 12.04%, 8.75% and 5.41%. Very high and phenomenal Seas are very rare in the Sea.

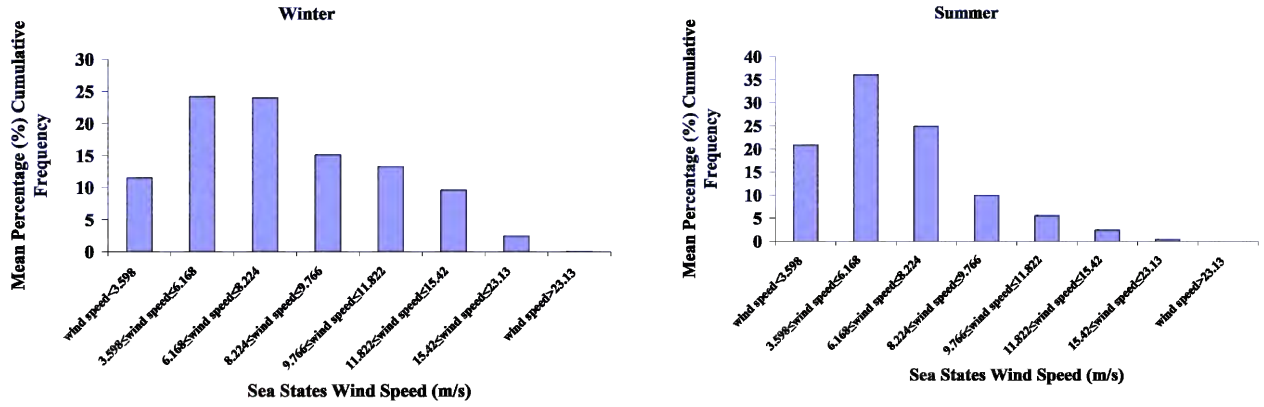
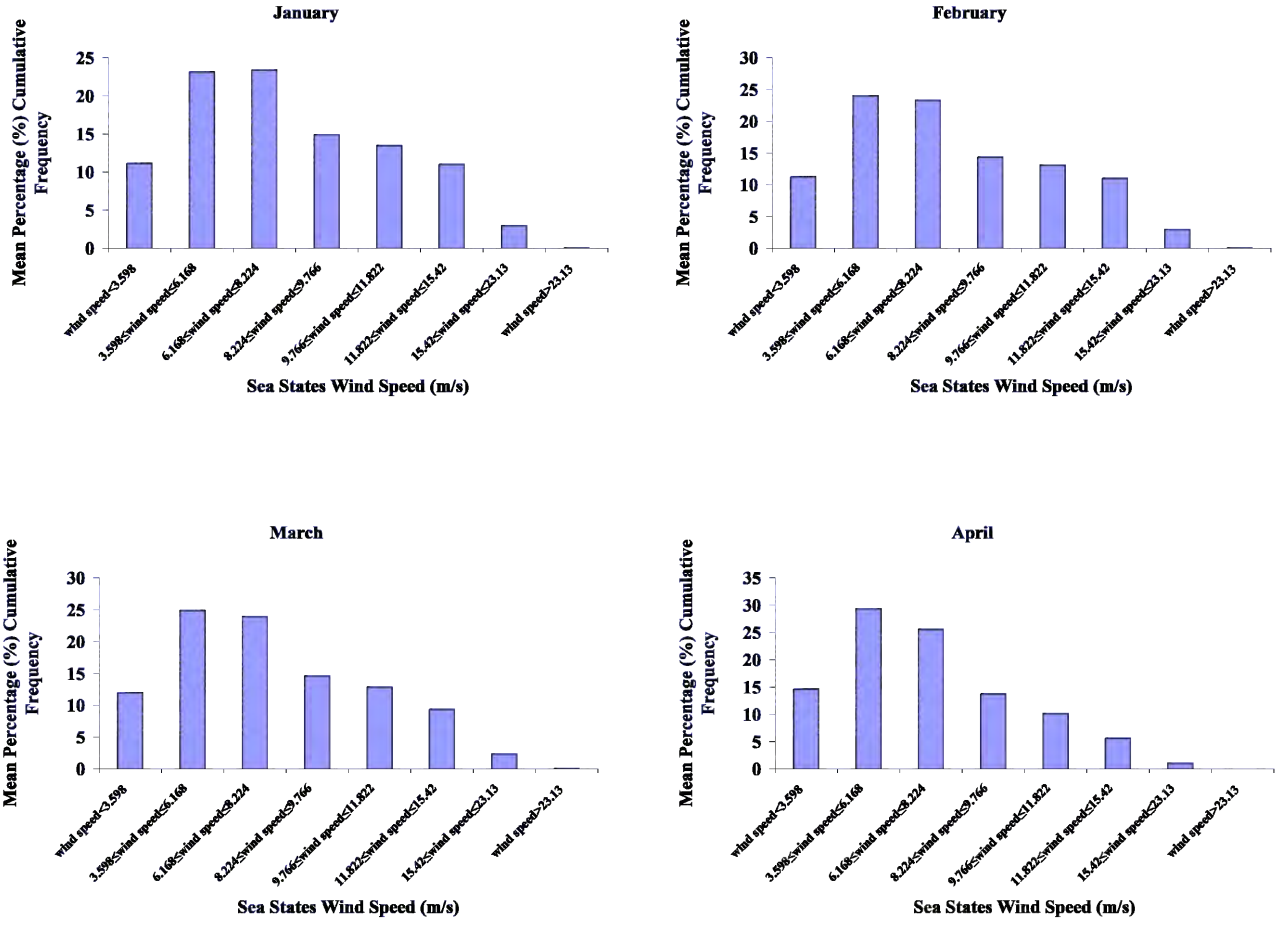
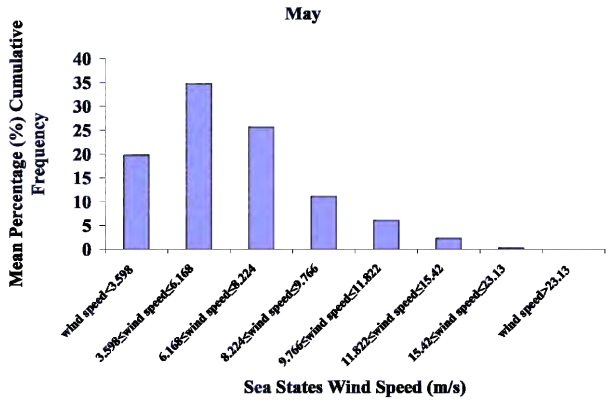
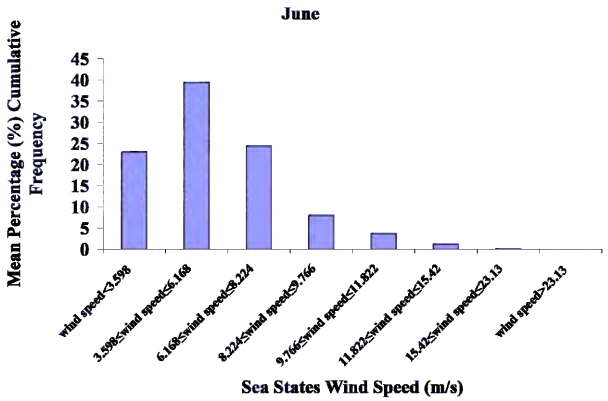
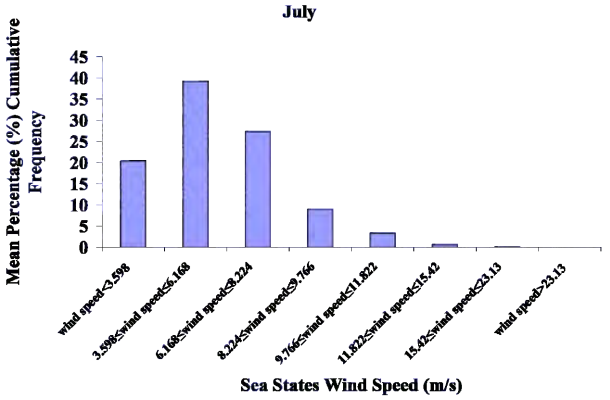


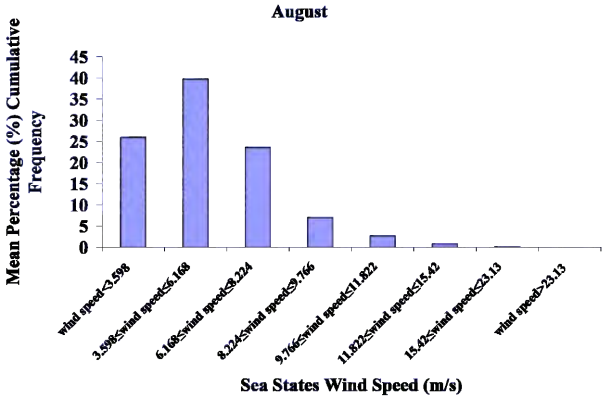

**Figure. IX.** Seasonal mean cumulative percentage frequency of *wind speed* for different Sea states in the Bermuda Sea.

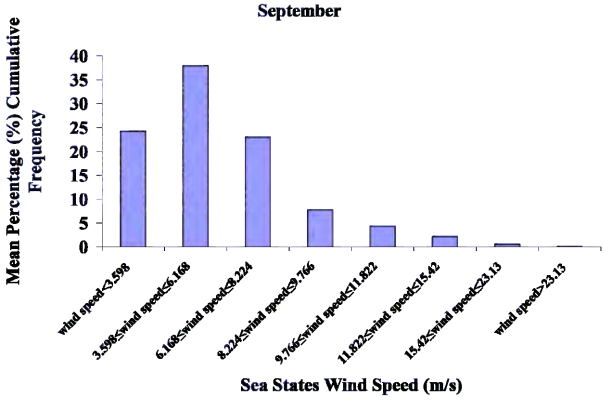


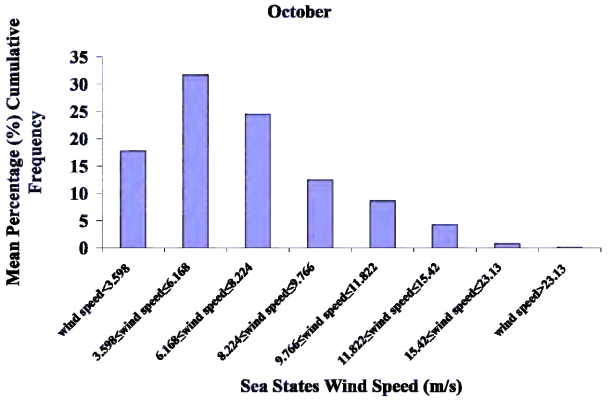

May
Mean Percentage (%) Cumulative Frequency
0
5
10
15
20
25
30
35
40
wind speed<3.598
3.598≤wind speed≤6.168
6.168≤wind speed≤8.224
8.224≤wind speed≤9.766
9.766≤wind speed≤11.822
11.822≤wind speed≤15.42
15.42≤wind speed≤23.13
wind speed>23.13
Sea States Wind Speed (m/s)


June
Mean Percentage (%) Cumulative Frequency
0
5
10
15
20
25
30
35
40
45
wind speed<3.598
3.598≤wind speed≤6.168
6.168≤wind speed≤8.224
8.224≤wind speed≤9.766
9.766≤wind speed≤11.822
11.822≤wind speed≤15.42
15.42≤wind speed≤23.13
wind speed>23.13
Sea States Wind Speed (m/s)


July
Mean Percentage (%) Cumulative Frequency
0
5
10
15
20
25
30
35
40
45
wind speed<3.598
3.598≤wind speed≤6.168
6.168≤wind speed≤8.224
8.224≤wind speed≤9.766
9.766≤wind speed≤11.822
11.822≤wind speed≤15.42
15.42≤wind speed≤23.13
wind speed>23.13
Sea States Wind Speed (m/s)


August
Mean Percentage (%) Cumulative Frequency
0
5
10
15
20
25
30
35
40
45
wind speed<3.598
3.598≤wind speed≤6.168
6.168≤wind speed≤8.224
8.224≤wind speed≤9.766
9.766≤wind speed≤11.822
11.822≤wind speed≤15.42
15.42≤wind speed≤23.13
wind speed>23.13
Sea States Wind Speed (m/s)


September
Mean Percentage (%) Cumulative Frequency
0
5
10
15
20
25
30
35
40
wind speed<3.598
3.598≤wind speed≤6.168
6.168≤wind speed≤8.224
8.224≤wind speed≤9.766
9.766≤wind speed≤11.822
11.822≤wind speed≤15.42
15.42≤wind speed≤23.13
wind speed>23.13
Sea States Wind Speed (m/s)


October
Mean Percentage (%) Cumulative Frequency
0
5
10
15
20
25
30
35
wind speed<3.598
3.598≤wind speed≤6.168
6.168≤wind speed≤8.224
8.224≤wind speed≤9.766
9.766≤wind speed≤11.822
11.822≤wind speed≤15.42
15.42≤wind speed≤23.13
wind speed>23.13
Sea States Wind Speed (m/s)

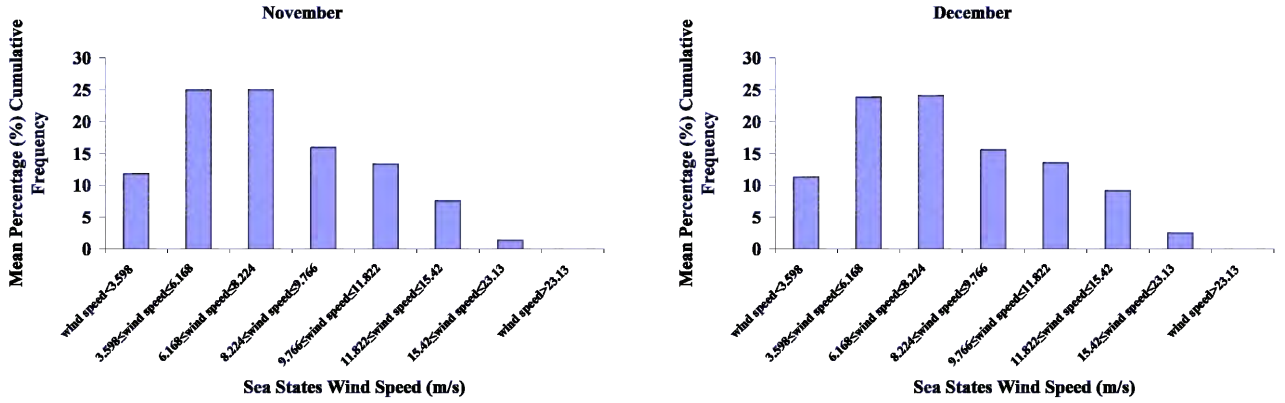



**Fig X.** Monthly mean cumulative percentage frequency of *wind speed* for different Sea states in the Bermuda Sea.

For the Seasonal Sea surface characteristics presented in Figure. IX, the slight Sea has the largest percentage frequencies of 24.2% and 36.01% both at winter and summer. The percentage frequencies of the rough, very rough and high Seas with respective frequencies of 15.11%, 13.3% and 9.6% are higher during winter than in summer. The smooth (wavelets) and moderate Seas showed higher frequencies of 20.81% and 24.86% in summer than in winter. For both Seasons, very high and phenomenal Seas had little or no occurrence.

The monthly mean characterization in Figure. X shows that the slight Sea generally has higher occurrence in all months except in November through January when the moderate Sea had higher frequencies which are respectively 24.99%, 24.11% and 23.4%. The slight Sea occurred most in June through August with respective frequencies of 39.43%, 39.2% and 39.7% and occurred least in December through February with respective frequencies of 23.81%, 23.12% and 23.98%. Regarding the rough and very rough Seas, the Sea appeared to be more turbulent in November through March. The Sea is smoother in May through September with respective frequencies of 19.74%, 23.02%, 20.4%, 25.92% and 24.21%. Higher frequencies (9.2%, 11.02%, 11.01% and 9.37%) occurred for high Sea in December through March. Very high and phenomenal Seas occurred on very rare occasions.

Figure XI presents the spatial characteristics of the cumulative percentage frequencies of wind speed for the different Sea conditions. It is observed that the smooth (wavelets) Sea occurred less than 30% in every region of the Sea. Slight traces of higher occurrences (40% -60%) are found in small regions along the coasts of Albemarle Sound and south of Bahamas. The slight Sea showed higher frequencies (35% -45%) in regions surrounding Miami, Bahamas and in few waters in the southern and northern regions of the Sea. Higher occurrences (30%-47%) of the moderate Sea dominate in the southern waters of the Sea. The largest occurrence (25%-28%) of the rough Sea is found in a small region south of Turks and Caicos Islands. The occurrence (12%-16%) of

### 3.4 Spatial Distribution of Sea States Using Wind Speed

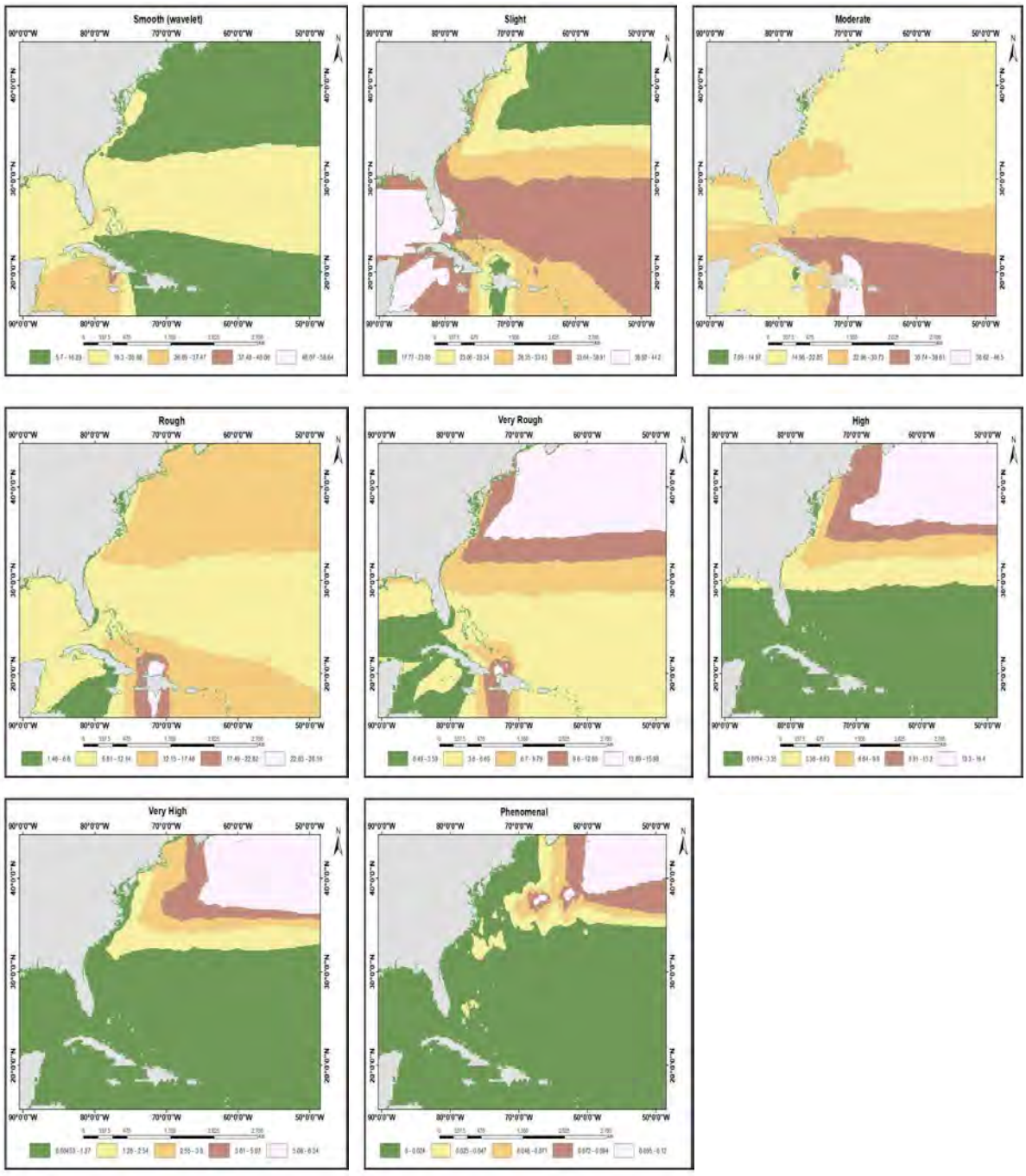



**Fig XI.** Spatial variation of the cumulative percentage frequency of *wind speed* for the various Sea states in the Bermuda Sea. Values on the vertical bars are in percentage.

the very rough Sea is higher in virtually every location in the northern region of the Sea and in few waters south of Turks and Caicos Islands. For the high and very high Seas, higher frequencies (14%-16%) and (5%-6.5%) are respectively found in the northeastern waters. There is very little or no occurrence (0.1%-0.13%) of phenomenal Sea in few waters in the northeastern part.

### 3.4 Spatial trends in Sea states using SWH

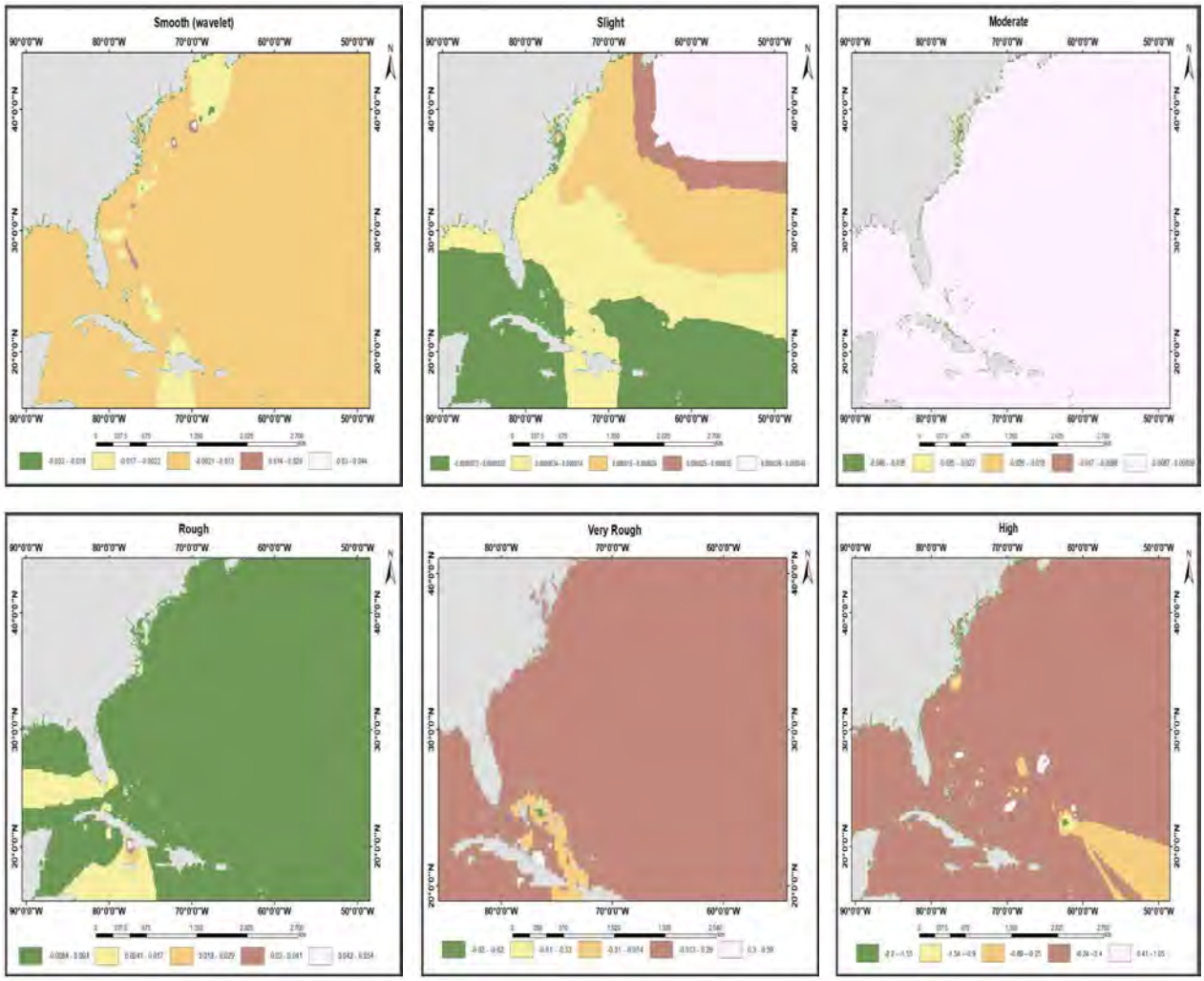



**Figure. XII.** Spatial variation of the linear trends for the various Sea states using SWH in the Bermuda Sea. Values on the vertical bars are in $myr^{-1}$.

The long-term spatial trends for the different Sea surface categories are presented in Figure XII. The calm (glassy), calm (rippled), very high and phenomenal Seas are not captured in this section since they are non significant in the linear trend analysis. Strong positive trends ( > $0.02myr^{-1}$) in smooth (wavelets) Sea are found in few waters north of Albemarle Sound and Miami. Insignificant and negative trends distribute in the rest regions of the Sea. The slight Sea exhibits the strongest trend of ($0.00003myr^{-1}$-$0.000045myr^{-1}$) in the northeastern part of the Sea but the trends are generally found to be insignificant. As for the moderate Sea, insignificant and negative trends dominate in every part of the Sea. Strong positive trends ( > $0.1myr^{-1}$) for the high Sea are seen in few regions in the central Bermuda Sea. Weaker trends dominate in the rest waters of the Sea.

The long-term linear trends for the different Sea surface categories, using the wind speed are presented in Figure XIII. Insignificant and negative trends in smooth (wavelets) and moderate, rough, high Seas dominate the Sea.

### 3.4 Spatial trends in Sea states using wind speed

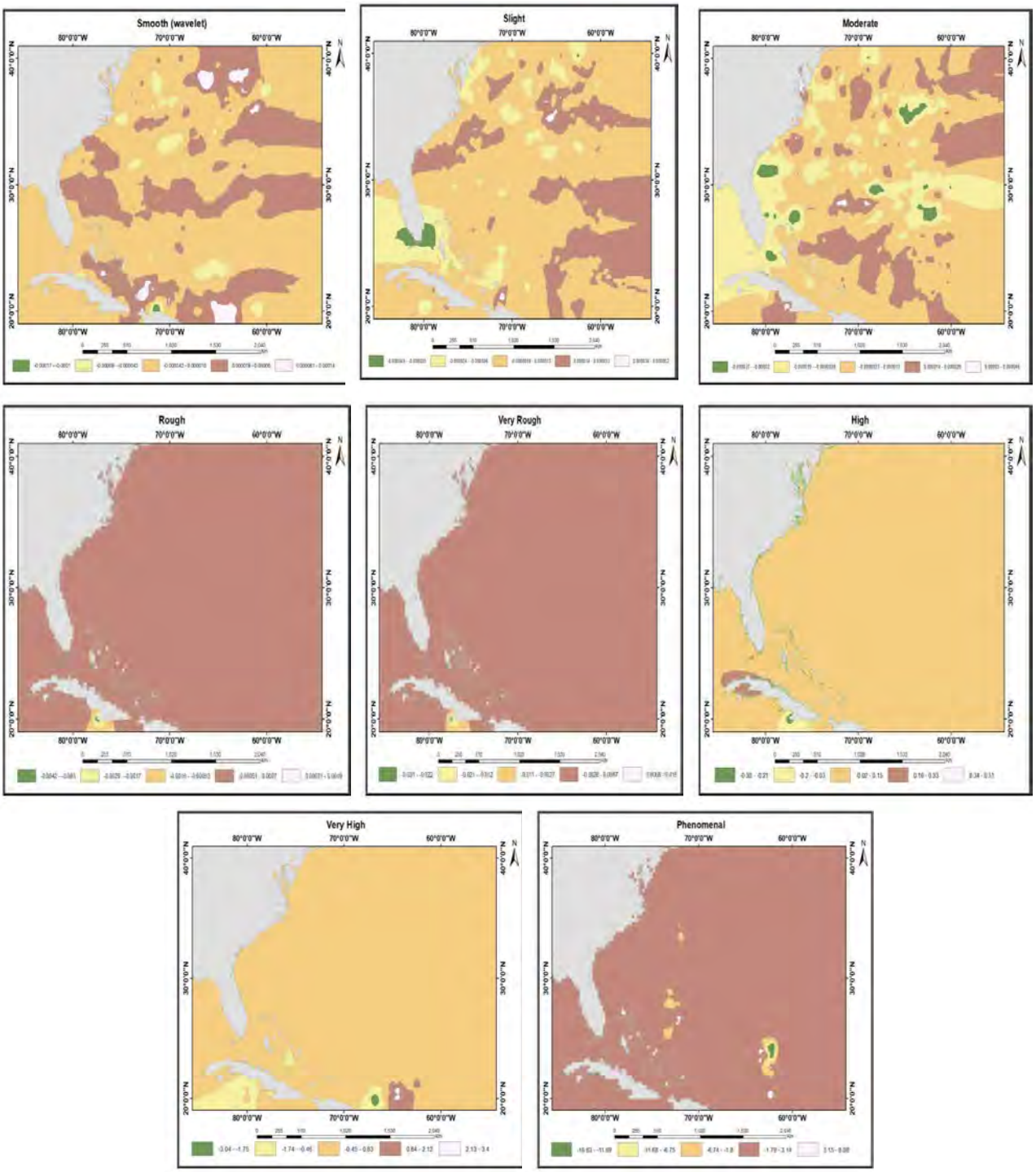



**Figure. XIII.** Spatial variation of the linear trends for the various Sea states using wind speed in the Bermuda Sea. Values on the vertical bars are in $myr^{-1}$.

Insignificant trends exist for the slight Sea in all regions of the Sea. Significant positive trends ($0.02ms^{-1}yr^{-1}$-$0.04ms^{-1}yr^{-1}$) in the very rough Sea are found in a very small region in the extreme southwest of Bermuda Sea. For the very high Sea, strongest positive trends ($1.5ms^{-1}yr^{-1}$-$4ms^{-1}yr^{-1}$) concentrate in a small region south of Turks and Carcois Islands. Also, strong positive trends ($1ms^{-1}yr^{-1}$-$1.4ms^{-1}yr^{-1}$) distribute in the sporadic waters in the southern Bermuda Sea, while weaker positive trends of approximately $0.2ms^{-1}yr^{-1}$ are found in the central and northern regions of the Sea. Insignificant and negative trends are seen in few waters in the southern Sea. The phenomenal Sea exhibits the strongest positive trend of up to $5ms^{-1}yr^{-1}$ in sporadic regions of the Sea. Insignificant and negative trends distribute in the rest regions of the Sea.

## 4.0 Conclusion

In this study, a thirty-seven (37) year data of SWH and wind speed derived from simulations were used to statistically investigate the Sea surface conditions in the Bermuda Sea. A characterization of the annual, Seasonal, and monthly average Sea surface characteristics based on these parameters were done. Results showed that in both cases, the slight and moderate Sea surface conditions prevailed in the Bermuda Sea. The Sea is generally rougher during winter than in summer. A spatial analysis of Sea surface using SWH showed that the smooth (wavelets) Sea occurred mostly (70%-85%) along the coasts of Albemarle Sound. The slight Sea had peak frequencies (60%-75%) along the western boundaries of the Sea. The moderate Sea occurred most (70%-80%) around Turks and Caicos Islands. Higher frequencies of 20%-27% and 8%-11% respectively for the rough and very rough Seas dominate in the northeastern waters. Also, higher frequencies of 1.75%-2.25% and 0.06%-0.08% respectively for the high and very high Seas dominate in sporadic waters in the northeastern part of the Sea. The calm (glassy), calm (rippled) and phenomenal Seas are rare. Spatial trend analysis revealed that strong positive trends ( $> 0.02myr^{-1}$) in smooth (wavelets) Sea are found in few waters north of Albemarle Sound and Miami. Trends greater than $0.1myr^{-1}$ for the high Sea are seen in few regions in the central Bermuda Sea. Insignificant and negative trends occurred for the other Sea states. Also, the spatial analysis of Sea states using wind speed showed that higher occurrences (40%-60%) of the smooth (wavelets) are seen in small regions along the coasts of Albemarle Sound and south of Bahamas. The slight Sea is higher (35%-45%) in regions surrounding Miami, Bahamas and in few waters in the southern and northern regions of the Sea. Higher occurrences (30%-47%) of the moderate Sea are found in the southern region of the Sea, while the largest occurrence (25%-28%) of the rough Sea is found in a small region beneath the Turks and Caicos Islands. The very rough Sea showed higher occurrence (12%-16%) in the northern Bermuda Sea and in few regions south of Turks and Caicos Islands. Higher frequencies of (14%-16%) and (5%-6.5%) respectively for the high and very high Seas, are found in the northeastern waters of the Sea. The phenomenal Sea is very rare. Analysis of the spatial trend showed that the very rough Sea exhibited strong positive trends between $0.02ms^{-1}yr^{-1}$ and $0.04ms^{-1}yr^{-1}$ in a small region in the extreme southwest of Bermuda Sea. The very high Sea showed trends >

$0.2ms^{-1}yr^{-1}$ in few waters in the southern Bermuda Sea and all through the central and northern regions of the Sea. The phenomenal Sea exhibits the strongest positive trend of up to $5ms^{-1}yr^{-1}$ in sporadic regions of the Sea. Insignificant and negative trends exist for the other categories of Sea.

## Conflicts of interest and funding

We have no conflicts of interest to disclose. This research did not receive any specific grant from funding agencies in the public, commercial, or not-for-profit sectors.

## Acknowledgements

We authors wish to acknowledge the kind effort of Mrs Oluchi Okere of the General Studies Department, Federal University of Technology, Akure, Nigeria for the language help provided and the proof reading of the manuscript. The effort of Dr. Kaiwen Zheng of the College of Oceanic and Atmospheric Sciences, Physical Oceanography Laboratory, Ocean University of China, towards data validation and simulation is also appreciated.

## References

**Alizadeh MJ, Kavianpour MR, Kamranzad B, Etemad-Shahidi A (2020).** A distributed wind downscaling technique for wave climate modeling under future scenarios. *Ocean Modelling, Volume* v.145, p.2020, https://doi.org/10.1016/j.ocemod.2019.101513.

**Alizadeh, M. J., Nourani, V., & Kavianpour, M. R. (2021).** A statistical framework to project wave climate and energy potential in the Caspian Sea: application of CMIP6 scenarios. *International Journal of Environmental Science and Technology*. v.19, p.2323–2336

Ardhuin, F., Stopa, J., Chapron, B., Collard, F., Husson, R., Jensen, R., Johannessen, J., Mouche, A., Passaro, M., Quartly, D., Swail, V., and Young, I. (2019). Observing sea states, *Frontiers in Marine Science* 6 (2019) Article 124, 29p.

**Bitner-Gregersen, E.M., Dong, S., Fu, T., Ma, N., Maisondieu, C., Miyake, R., and Rychlik, I. (2016).** Sea state conditions for marine structures' analysis and model tests. *Ocean Engineering*, v.119, p.309–322
http://dx.doi.org/10.1016/j.oceaneng.2016.03.024

**Caires, S., Swail, V., Wang, X. (2006).** Projection and analysis of extreme wave climate. *J. Climate* v.19 (21), p.5581-5605

**Casas-Prat, M., Wang, X., Swart, N. (2018).** CMIP5-based global wave climate projections including the entire Arctic Ocean. *Ocean Model.* vol.123, 66–85.

**Chalikov, D.V., Belevich, M., and Yu. (1993).** One-dimensional theory of the wave boundary layer. *Bound Layer Meteor.*, v.63, p.65–96.

**Dodet, G., Piolle, J-F., Quilfen, Y., Abdalla, S., Accensi, M., Ardhuin, F., Ash, E.,**

**Bidlot, J-R., Gommenginger, C., Marechal, G., Passaro, M., Quartly, G., Stopa, J., Timmermans, B., Young, I., Cipollini, P., and Donlon, C. (2020).** The Sea State CCI dataset v1: towards a sea state climate data record based on satellite observations. *Earth Syst. Sci. Data*, v.12, p. 1929–1951, https://doi.org/10.5194/essd-12-1929-2020.

**Hanafin, J.A., Quilfen, Y., Ardhuin, F., Sienkiewicz, J., Queffeulou, P., Obrebski, M., Chapron, B., Reul, N., Collard, F., Corman, D., B. De Azevedo, E., Vandemark, D., and Stutzmann, E. (2012).** Phenomenal sea states and swell from a North Atlantic storm in February 2011. *Bul Am Meteorol Soc*. v.93(12), p 1825–1832 https://doi.org/10.1175/BAMS-D-11-00128.2.

**Hemer, MA., Katzfey, J., Trenham, CE. (2013).** Global dynamical projections of surface ocean wave climate for a future high greenhouse gas emission scenario. *Ocean Model*. v.70, p.221–245.

**Hemer M.A. and Trenham CE (2016)** Evaluation of a CMIP5 derived dynamical global wind wave climate model ensemble. *Ocean Modell*. v.103, p. 190–203 https://doi.org/10.1016/j.ocemod.2015.10.009

**Innocenti, A., Onorato, M., and Brandini, C. (2021).** Analysis of Dangerous Sea States in the Northwestern Mediterranean Area. *J. Mar. Sci. Eng*. v.9(4), p.422. https://doi.org/ 10.3390/jmse9040422.

**Kamranzad, B., Etemad-Shahidi, A., Chegini, V., Yeganeh-Bakhtiary, A., 2015.** Climate change impact on wave energy in the Persian Gulf. *Ocean Dyn*. v.65, p.777–794.

**Lemos G, Semedo A, Dobrynin M, Behrens A, Staneva J, Bidlot J-R, Miranda PM (2019).** Mid-twenty-frst century global wave climate projections: results from a dynamic CMIP5 based ensemble. Global and Planetary Change. v.172, 69–87. https://doi.org/10.1016/j.gloplacha.2018.09.011

**MacHutchon K. R, (2005).** A review of statistical methods of analysis applied to the wave climate in the area of the Agulhas Bank in the Southern Indian Ocean, *WIT Transactions on The Built Environment, WIT Press*, v.78, p.225–234 https://www.witpress.com/Secure/elibrary/papers/CE05/CE05020FU.pdf.

**Moeini M, and Etemad-Shahidi A (2007).** Application of two numerical models for wave hindcasting in Lake Erie. *Appl Ocean Res* v.29, p.137–145.

**Nguyen, T.D., Sorensen, A.J., and Quek, S.T. (2007).** Design of hybrid controller for dynamic positioning from calm to extreme Sea conditions. *Elsevier, Automatica*

v.43(5), p.768–785. doi:10.1016/j.automatica.2006.11.017.

**Nielsen, U.D. (2017).** A concise account of techniques available for shipboard sea state estimation. *Ocean Engineering* v.129, p.352–362.

**Nielsen, U.D., and Dietz, J. (2020).** Estimation of sea state parameters by the wave buoy analogy with comparisons to third generation spectral wave models, *Ocean Engineering* v.216, p.107781.

**Osinowo, A.A., Lin, X., Zhao, D., and Wang, Z. (2017).** Statistical Analyses of Sea State Conditions in South China Sea. *J. Ocean Univ. China* (Oceanic and Coastal Sea Research) v.16(3), p.357-369D O I 10.1007/s11802-017-3188-9

**Osinowo, A.A., Okogbue, E.C., Adefisan, E.A., and Ogunrayi, O.A. (2018).** On the statistical characterization of Sea surface conditions in the mid Atlantic. *Modeling Earth Systems and Environment*. v.4(4), p.1487–1507 https://doi.org/10.1007/s40808-018-0494-1.

**Park, J-H., Bae, J-H., and Baeg, M-H.(2017).** Estimation of Fluctuation Characterizations by USV-Operation Simulations in Sea State. *Hindawi Modelling and Simulation in Engineering* v.2017, Article ID 1305752, p.1–8 https://doi.org/10.1155/2017/1305752

**Semedo, A., Weisse, R., Behrens, A., Sterl, A., Bengtsson, L., Günther, H. (2012).** Projection of global wave climate change toward the end of the twenty-first century. *J. Clim.* v.26, p.8269–8288.

**Semedo, A., Dobrynin, M., Lemos, G., Behrens, A., Staneva, J., de Vries, H., Sterl, A., Bidlot, J.-R., Miranda, P., Murawski, J. (2018).** Cmip5-derived single-forcing, single-model, and single-scenario wind-wave climate ensemble: configuration and performance evaluation. *J. Mar. Sci. Eng*. v.6(90), p1–28 .

**Thomson, J., Fan, Y., Stammerjohn, S., Stopa, J., Erick Rogers, W., Girard-Ardhuin, F., Ardhuin, F., Shen, H., Perrie, W., Shen, H., Ackley, S., Babanin, A., Liu, Q., Guest, P., Maksym, T., Wadhams, P., Fairall, C., Persson, O., Doble, M., Graber, H., Lund, B., Squire, V., Gemmrich, J., Lehner, S., Holt, B., Meylan, M., Brozena, J., and Bidlot, J-R. (2016).** Emerging trends in the sea state of the Beaufort and Chukchi seas. *Ocean Modelling*. v.105, p.1–12..

**Tolman, H.L. (1999).** User Manual and System Documentation of WAVEWATCH-III Version 1.18. *Washington*. p.56.

**Tolman, H.L. (2009).** User Manual and System Documentation of WAVEWATCH-III Version 3.14. *NOAA/NWS/NCEP/MMAB Technical Note, Washington*, p.194.

**Tolman, H.L., and Chalikov, D.V. (1996).**

Source terms in a third generation wind-wave model. *J. Phys. Oceanogr*., v.26, p.2497–2518.

**Vanem, E. (2015).** Non-stationary extreme value models to account for trends and shifts in the extreme wave climate due to climate change. *Appl. Ocean Res*. V.52, p.201–211.

**Wandres, M., Pattiaratchi, C., Hemer, M.A. (2017).** Projected changes of the southwest Australian wave climate under two atmospheric greenhouse gas concentration pathways. *Ocean Model*. V.117, p.70–87.

**Wang, X., Swail, V., Cox, A., (2010).** Dynamical versus statistical downscaling methods for ocean wave heights. *Int. J. Climatol*, v.30 (3), p.317-332.

**Wang, X.L., Feng, Y., Swail, V.R., (2014).** Changes in global ocean wave heights as projected using multimodel CMIP5 simulations. *Geophys. Res. Lett*. v. 41, p.1026-1034.

**Wang, L., Perrie, W., Long, Z., Blokhina, M., Zhang, G., Toulany, B., Zhang, M. (2018).** The impact of climate change on the wave climate in the Gulf of St. Lawrence. *Ocean Model*. v.128, p.87–101.

**Wilks, D.S. (1995).** Statistical Methods in the Atmospheric Sciences: An Introduction. *Academic Press, San Diego, Calif, USA*.p.5

**Zhang, Z., and Li, X-M. (2017).** Global ship accidents and ocean swell-related sea states. *Nat. Hazards Earth Syst. Sci.*, v.17(11), p.2041–2051. https://doi.org/10.5194/nhess-17-2041-2017